

This PDF file is subject to the following conditions and restrictions:

Copyright © 2006, The Geological Society of America, Inc. (GSA). All rights reserved. Copyright not claimed on content prepared wholly by U.S. government employees within scope of their employment. Individual scientists are hereby granted permission, without fees or further requests to GSA, to use a single figure, a single table, and/or a brief paragraph of text in other subsequent works and to make unlimited copies for noncommercial use in classrooms to further education and science. For any other use, contact Copyright Permissions, GSA, P.O. Box 9140, Boulder, CO 80301-9140, USA, fax 303-357-1073, editing@geosociety.org. GSA provides this and other forums for the presentation of diverse opinions and positions by scientists worldwide, regardless of their race, citizenship, gender, religion, or political viewpoint. Opinions presented in this publication do not reflect official positions of the Society.

Magma mixing and mingling in the Grayback pluton, Klamath Mountains, Oregon

Kenneth Johnson*

*Department of Natural Sciences, University of Houston–Downtown,
1 Main Street, Houston, Texas 77002, USA*

Calvin G. Barnes

Department of Geosciences, Texas Tech University, Lubbock, Texas 79409, USA

ABSTRACT

The 160-Ma Grayback pluton provides ample evidence for the role of mantle-derived magmas in the crystallization history of the magma chamber. Mafic magmas tapped several distinct mantle sources, and evidence for magma mixing is manifest in (1) widespread mafic enclave swarms in which basaltic magma mingled with basaltic to andesitic magma, (2) late-stage granodioritic dikes containing pillow-shaped enclaves of basalt and hybrid andesite, and (3) late-stage tonalitic dikes including microdioritic enclaves contained within a dark-colored hybrid matrix. These magma-mingling zones reflect large-scale magma mixing processes in the Grayback system. Much of the compositional variation among Grayback main-stage samples was apparently produced by magma mixing between mafic and intermediate magmas similar to those exposed in some of the mafic enclave swarms. Mixing between basaltic and granitic end-members at deeper levels in the Grayback magma chamber produced hybrid andesite. Enclaves of basalt and hybrid andesite are observed in late-stage granodioritic dikes that cut the mafic enclave swarms. Mingling between partially crystalline basaltic and tonalitic mushes, resulting in a mega- and microscopically complex hybrid, is observed in the late-stage tonalitic dikes. Few Grayback main-stage samples were apparently produced in this manner.

The Grayback pluton is one of several similar-aged plutons in the Wooley Creek suite, in which mafic magma played a prominent role in petrogenesis. The Grayback system is unusual in that mafic magmas from several obviously different sources were present throughout its crystallization history. This circumstance probably resulted from its position in an extensional, back-arc setting.

Keywords: magma mixing, magma mingling, Klamath Mountains, hybridization, enclave

*E-mail: JohnsonK@uhd.edu.

Johnson, K., and Barnes, C.G., 2006, Magma mixing and mingling in the Grayback pluton, Klamath Mountains, Oregon, in Snoke, A.W., and Barnes, C.G., eds., Geological studies in the Klamath Mountains province, California and Oregon: A volume in honor of William P. Irwin: Geological Society of America Special Paper 410, p. 247–267, doi: 10.1130/2006.2410(12). For permission to copy, contact editing@geosociety.org. ©2006 Geological Society of America. All rights reserved.

INTRODUCTION

Most Jurassic plutons in the Klamath Mountains province occupy “belts” or suites that are defined by relatively narrow age ranges, geographic settings, and exposed rock types (Hotz, 1971; Irwin, 1985; Irwin and Wooden, 1999). More recent work has shown that plutons within belts share broadly similar petrogenetic histories. This commonality is particularly the case for plutons within the Ironside Mountain batholith (Barnes et al., this volume, Chapter 10), the Wooley Creek suite (Barnes, 1983; Barnes et al., 1986, 1995; Gribble et al., 1990), which now includes several plutons from the Grayback belt of Irwin (1985), and for Late Jurassic to Early Cretaceous tonalitic and trondhjemitic intrusions in the eastern Klamath Mountains (Barnes et al., 1996; Allen and Barnes, this volume). Plutons within the Wooley Creek suite evolved largely as open systems, involving assimilation of crustal rocks, recharge of mantle-derived magma, and/or mixing between mantle and crustal melts. Detailed study of such open systems provides information about the source(s) of magmas, the nature of the crust through which they ascended, and the timing of magma mixing/mingling events.

Magma mixing is commonly invoked to explain compositional variations in plutonic and volcanic suites from a variety of tectonic environments. Evidence for the interaction of magmas at the outcrop scale is found in banded pumice and mafic magmatic enclaves. Mafic magmatic enclaves (hereafter referred to as “enclaves”) are common and often widespread features of both volcanic and plutonic rocks, and there is general consensus that they represent blobs of mafic magma that were rapidly undercooled when brought into contact with cooler, more felsic magma. Striking examples of basaltic “pillows” in felsic rocks have been presented that leave little doubt, at least at the outcrop scale, as to their magmatic origin (e.g., Wiebe, 1991; Wiebe et al., 2001). Often the petrogenetic significance of enclaves is uncertain, other than to indicate that mafic magma was present during the crystallization history of the pluton. If the presence of enclaves in mingling zones can be used to demonstrate that magma mixing was important in the compositional evolution of a magma, then such features may provide information about the physical and chemical processes involved in mixing.

The late Middle Jurassic Grayback pluton in southwestern Oregon is a large, reversely zoned member of the Wooley Creek plutonic suite. Magma-mingling zones are extensively exposed throughout the pluton. They feature a wide variety of intermingled rock types and provide evidence for mingling throughout the pluton’s history. The observed mixing and mingling relationships indicate that mafic mantle-derived magmas were not only present, but played an important role in the evolution of the Grayback pluton. The Grayback pluton is not unique in this respect; all plutons in the Wooley Creek belt exhibit characteristics of open-system behavior and the involvement of mafic magmas during their crystallization histories (Barnes et al., 1986, 1987; Gribble et al., 1990). However, the Grayback pluton is particularly well suited for such study, be-

cause magma-mixing processes were arrested in situ in a variety of mixing stages and involved a range of end-member compositions. In this chapter, we describe the range of mingling zones in the Grayback pluton and demonstrate their utility as small-scale analogues to pluton-wide processes. We then discuss the tectonic conditions under which the Grayback system evolved, conditions that may have allowed for widespread mixing and mingling behavior. In the following text, “mixing” refers to the process of blending two or more magmas together to form reasonably uniform hybrid magma, and “mingling” refers to incomplete mixing in which end-members are physically distinct, typically resulting in enclave-bearing rocks or mingling zones.

REGIONAL GEOLOGY

The Klamath Mountains of northwestern California and southwestern Oregon comprise an arcuate assemblage of four lithotectonic terranes, which represent fragments of oceanic crust and island arcs that were accreted to the western margin of North America during Late Paleozoic through Middle Mesozoic time (Irwin, 1981). These units are, from east to west and from structurally highest to lowest, the eastern Klamath, central metamorphic, western Paleozoic and Triassic, and the western Jurassic terranes or belts (Fig. 1). The belts are separated by east-dipping thrust faults, so that structurally higher rocks were thrust over generally younger rocks to the west. Thrusting of the western Paleozoic and Triassic over the western Jurassic belt along the Orleans fault was responsible for some of the deformation associated with the Nevadan orogeny at ca. 152–150 Ma (Saleeby et al., 1982; Harper and Wright, 1984).

Calc-alkaline and calcic magmatism occurred during Jurassic and Early Cretaceous times. Barnes et al. (1992a) showed that pre-Nevadan plutons are chemically and isotopically distinct from post-Nevadan ones, reflecting a change from largely mantle-derived magmas to those formed by crustal melting in response to underthrusting of ophiolitic rocks beneath older terranes to the east (Barnes et al., 1992b, 1996). A sample from the Grayback pluton main stage yielded a zircon U-Pb age of 160 ± 2 Ma (Yule et al., this volume), whereas late-stage samples yielded a zircon U-Pb age of 157 ± 2 Ma (Yule et al., this volume) and a hornblende $^{40}\text{Ar}/^{39}\text{Ar}$ age of 157.3 ± 1.4 Ma (Hacker et al., 1995). These ages place Grayback magmatism within the age range of plutons belonging to the 165- to 156-Ma “Wooley Creek suite” that includes the Wooley Creek batholith and Slinkard pluton (Barnes et al., 1986), the Russian Peak pluton (Cotkin and Medaris, 1993), the Ashland pluton (Gribble et al., 1990), and the English Peak pluton (Schmidt, 1994). To the west of the Wooley Creek belt are the 165- to 159-Ma Josephine ophiolite (Wyld and Wright, 1988; Harper et al., 1994) and 161- to 156-Ma Rogue–Chetco volcanic arc complex (Garcia, 1982; Yule et al., this volume).

The Grayback pluton intruded rocks of the Rattlesnake Creek and western Hayfork terranes, the westernmost of four

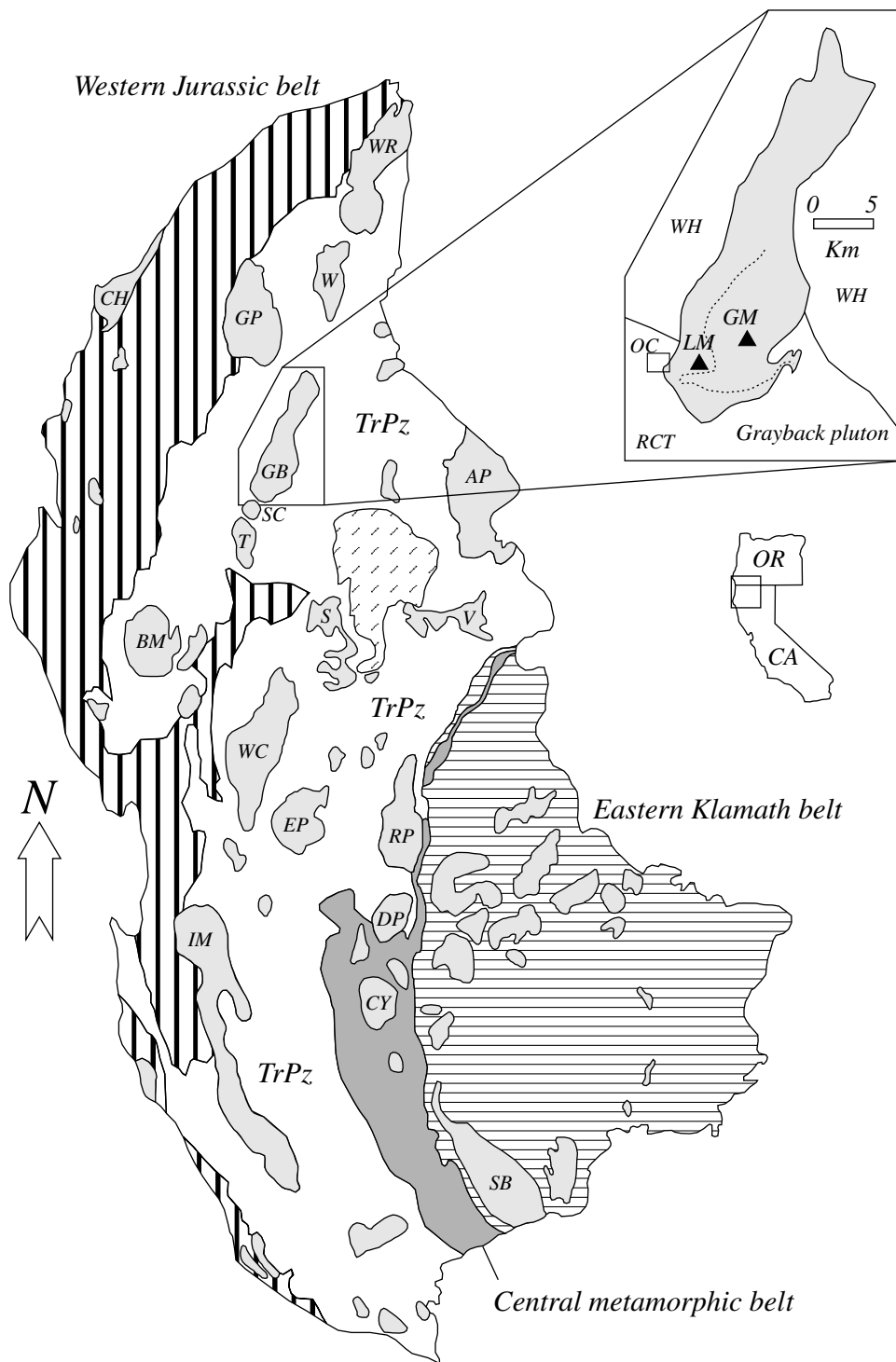


Figure 1. Geologic map of the Klamath Mountains showing boundaries between lithotectonic belts and locations of Jurassic and Cretaceous plutons. Inset shows locations of Lake Mountain (LM) and Grayback Mountain (GM) within the Grayback pluton. Square labeled "OC" represents the approximate locality of Oregon Caves National Monument. Thin dotted line within the Grayback pluton separates quartz-poor lithologies in the interior from quartz-rich ones along the margin (Barnes et al., 1995). AP—Ashland pluton; BM—Bear Mountain intrusive complex; CH—Chetco intrusive complex; CY—Canyon Creek pluton; DP—Deadman Peak pluton; EP—English Peak pluton; GB—Grayback pluton; GP—Grants Pass pluton; IM—Ironsides Mountain batholith; RCT—Rattlesnake Creek terrane; RP—Russian Peak pluton; S—Slinkard pluton; SB—Shasta Bally pluton; SC—Sucker Creek pluton; T—Thompson Ridge pluton; TrPz—western Paleozoic and Triassic composite belt; V—Vesa Bluffs pluton; WC—Wooley Creek batholith; WH—western Hayfork terrane; WR—White Rock pluton. Simplified from Irwin (1985).

terrane of the western Paleozoic and Triassic belt (Irwin, 1972; Donato et al., 1996; Ernst, 1998). The Grayback pluton is the largest of a linear, north–northeast-trending chain of four coeval plutons (ca. 161–160 Ma; Yule et al., this volume) that consists of the Weimer, Grayback, Sucker Creek, and Thompson Ridge plutons. The host rocks that separate these plutons are essen-

tially dike swarms with as much as 50% dike rock (Barnes et al., 1995; Donato et al., 1996). The presence of mafic dike swarms along the southern edge of the Grayback pluton, evidence for contemporaneous normal faulting, and its setting inboard of the coeval Rogue–Chetco arc led Barnes et al. (1995) to conclude that it was emplaced in a back-arc setting.

SAMPLE PREPARATION AND ANALYSIS

Samples were crushed and powdered in tungsten carbide and alumina shatterboxes. All samples were analyzed by inductively coupled plasma atomic emission spectrometry (ICP-AES) at Texas Tech University following methods described in Shannon (1994). Rare earth elements (REEs) were separated using the cation exchange elution method of Shannon (1994) and then analyzed by ICP-AES. Rubidium abundances were determined by flame atomic emission.

Mineral compositions were determined with a JEOL JXA-733 electron probe microanalyzer at Southern Methodist University, Dallas, Texas. Operating conditions were 15-kV accelerating potential, 20-nA beam current, and a 10- μ m spot, defocused to 20 μ m for plagioclase. Online corrections were made with the Bence-Albee procedure, and a suite of natural and synthetic minerals and glasses was used as standards.

GEOLOGY OF THE MAGMA-MINGLING ZONES

The main stage of the Grayback pluton consists of tonalite, quartz diorite, gabbro, and norite that were intruded by syn-plutonic noritic and gabbroic magmas, some of which resulted in widely dispersed enclaves throughout the pluton (referred to as "main-stage enclaves"). Late-stage activity was characterized by the intrusion of tonalitic and granodioritic dikes, many of which were enclave bearing. Detailed discussions of the geology and petrology of the Grayback pluton were presented in Godchaux (1969) and Barnes et al. (1995).

This study focuses on three types of magma-mingling zones in the Grayback pluton: (1) large, widespread swarms of mafic enclaves in a mafic to intermediate host; (2) late-stage granodioritic dikes containing pillow-shaped basaltic and andesitic enclaves; and (3) late-stage tonalitic dikes containing microdioritic enclaves enclosed in an intermediate matrix.

Mafic Enclave Swarms

Field Observations. These swarms consist of microgabbroic enclaves in gabbroic to dioritic host rocks. They are exposed on Lake Mountain and the ridge extending north from Grayback Mountain (Fig. 1). Some can be traced laterally for several hundred meters. They are complex intrusive zones within the main stage of the pluton and are intruded by coarse-grained hornblende gabbro and enclave-bearing felsic dikes.

Individual enclaves range from <1.0 cm to >2.5 m in longest dimension. Enclaves are generally lens-shaped and oriented parallel or subparallel to foliation in the host (Fig. 2A). In some places, enclaves constitute >90% of outcrop area and are separated by a thin septum (<0.5 cm) of host rock. The enclave boundaries are sharp and well defined, but lack the fine-grained "chilled" margins suggestive of rapid undercooling of the enclave magma.

On Grayback Mountain, enclaves are generally flattened at the margins of the mingling zones with aspect ratios approach-

ing 35:1, whereas in the center of the zone, aspect ratios are estimated to be <10:1. The enclaves are plastically deformed around brittle xenoliths, resulting in pressure shadows in which prismatic hornblende is randomly oriented. Elsewhere in the mingling zones, hornblende is parallel to the foliation.

Veins of the host rock, generally <0.5 cm in width, are common in most enclaves. However, most do not penetrate the entire enclave, but pinch out. These veins are generally parallel to the foliation of the host from which they originate and to the direction of enclave elongation (Fig. 2B). Aggregates of coarse-grained plagioclase and poikilitic hornblende, as much as 1.5 cm in length, are common throughout the finer-grained enclaves. The long axes of these aggregates are parallel to the foliation in the host and to the veins of host within the enclaves. They are commonly collinear with pinched out veins (Fig. 2C and D).

Petrography. The host rocks to these enclave swarms are hornblende norite (on Grayback Mountain) and biotite-hornblende quartz gabbro (on Lake Mountain). Host rocks consist of euhedral to subhedral, reversely to normally zoned plagioclase (An_{48-63}) + magnesio-hornblende ($Mg/[Mg + Fe] = 0.52-0.62$) + Fe-Ti oxides \pm orthopyroxene ($En_{53}Fs_{47}Wo_0$ to $En_{46}Fs_{52}Wo_2$) \pm biotite \pm quartz (Johnson, 1991). Titanite and zircon are minor accessories, whereas apatite is common. Hornblende is prismatic or poikilitic, with inclusions of plagioclase, apatite, and oxides. Minor late-stage cummingtonite is associated with hornblende.

Enclaves are micronorite (Grayback Mountain) and biotite hornblende quartz microgabbro (Lake Mountain). They have the same mineral assemblages as their respective hosts. Plagioclase compositions in the enclaves reach An_{69} , whereas hornblende and orthopyroxene compositions are similar to those in host rocks (Johnson, 1991). Plagioclase xenocrysts from the host are strongly zoned and are partially resorbed and embayed by quartz. Hornblende in the quartz microgabbro is prismatic, but it forms rims around pyroxene grains in the micronoritic enclaves. Aspect ratios of apatite in the enclaves rarely exceed 5:1 and are very similar to those in the host.

In thin section, enclaves typically exhibit a well-developed lamination defined by the parallel alignment of plagioclase laths (Fig. 2E), although enclaves with little or no lamination were observed. Lamination in the enclaves is generally parallel to the enclave/host interface, and may be deflected around mineral aggregates and xenocrysts from the host (Fig. 2F).

Late-Stage Granodioritic Dikes

Field Observations. Granodioritic dikes containing basaltic and andesitic "pillows" were studied at several localities including Lake Mountain summit, the U.S. Forest Service Boundary Trail south of Grayback Mountain, and along logging roads east of Oregon Caves National Monument in the southern portion of the pluton.

Basaltic enclaves are fine-grained, dark green to gray mafic pillowlike blobs that range from a few centimeters to slightly less than one meter in diameter. The basalt-granodiorite inter-

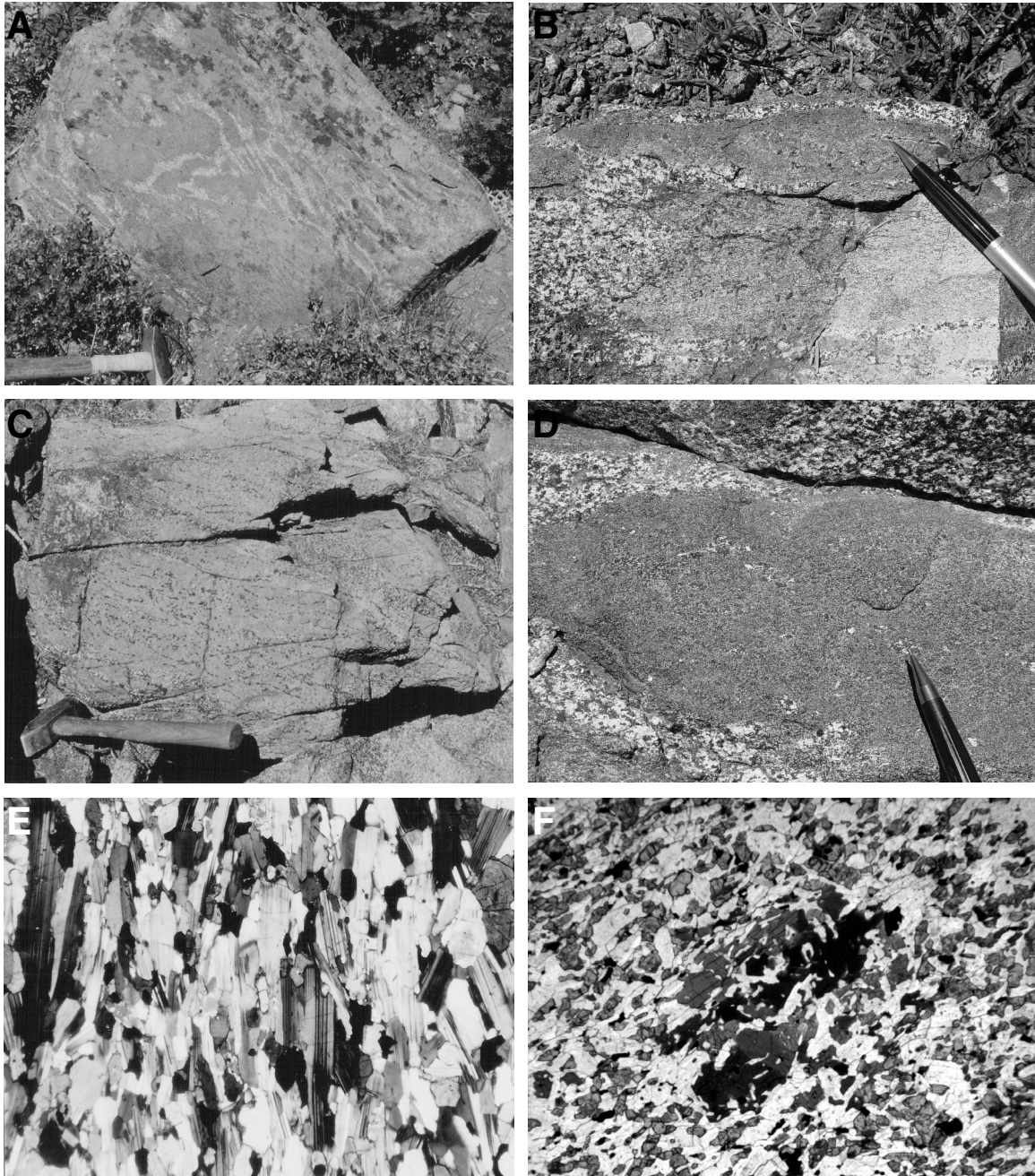


Figure 2. Photographs and photomicrographs of enclaves in the mafic enclave swarms. (A) Tightly packed enclaves of all sizes showing plastic behavior and high degree of elongation. (B) Coarse-grained vein of host material in fine-grained enclave. Vein terminates near tip of pencil. (C) Trails of hornblende xenocrysts in pyroxene-rich enclaves. Xenocryst trails are oriented parallel to lamination in the enclaves and foliation in the host. (D) Remnants of host vein material, now manifest as plagioclase and hornblende xenocrysts, within pyroxene-rich enclave. (E) Pronounced lamination in pyroxene-rich enclave defined by orientation of plagioclase laths (field of view is 6.0 mm). (F) Hornblende xenocryst in pyroxene-rich enclave. Plagioclase laths (white) and pyroxene grains (gray) are deflected around xenocryst (mostly extinct; field of view is 6.0 mm).

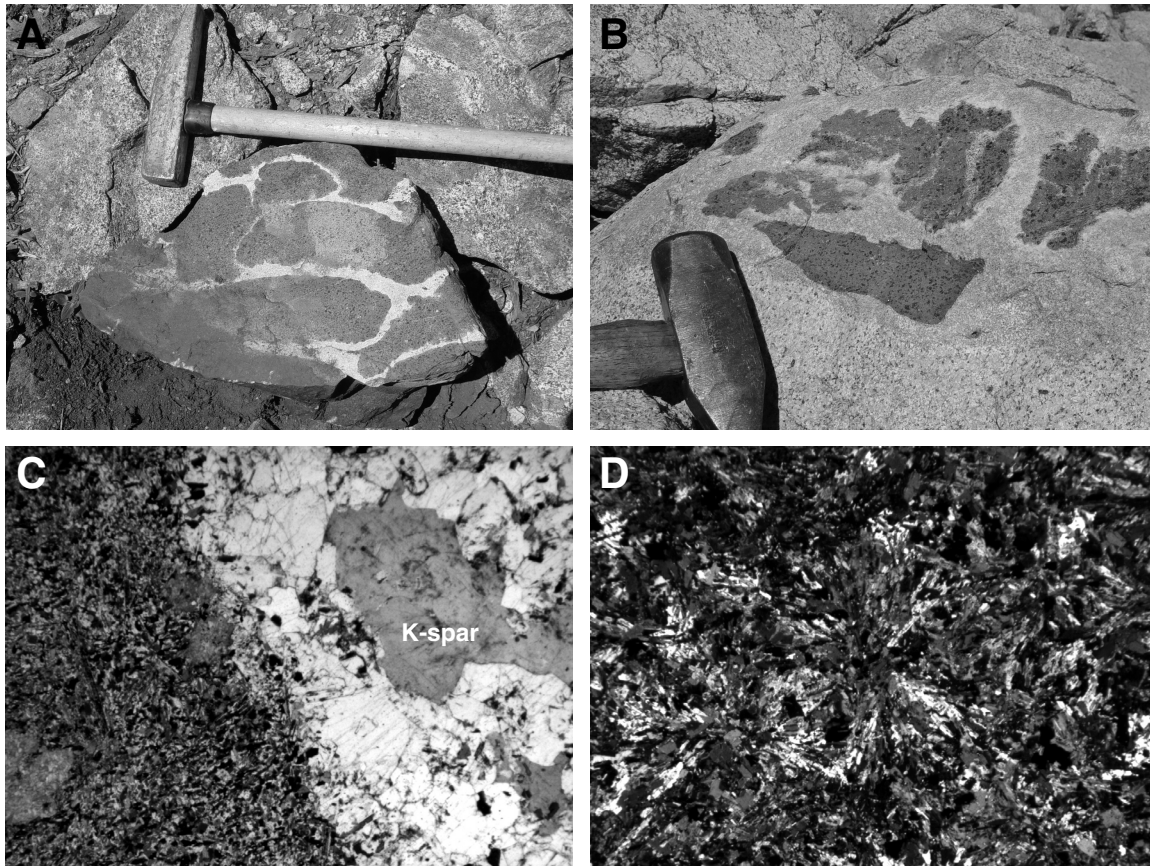


Figure 3. Photographs and photomicrographs of enclaves in late-stage granodioritic dikes. (A) Basaltic pillows in float block of granodiorite. Note the close-packed nature of the enclaves. (B) Thin trondhjemitic haloes surrounding basaltic enclaves. Haloes are lacking in K-feldspar and biotite. (C) Sharp interface between basaltic enclave (left) and granodioritic host (right; field of view is 6.0 mm). (D) Radiating plagioclase laths in hybrid andesitic enclave (field of view is 6.0 mm).

face is generally very sharp and convex toward the host (Fig. 3A), and the enclaves lack a preferred orientation. The enclaves are commonly enveloped by trondhjemitic zones (Fig. 3B) ~0.75 cm wide that lack K-feldspar and biotite. On fresh enclave surfaces, clots of randomly oriented plagioclase phenocrysts and clots of actinolitic hornblende 2–3 mm in length are visible.

Andesitic enclaves are less abundant than basaltic ones. They are fine-grained, pale-green, and intermediate in color between the basaltic pillows and granodioritic host. These enclaves are coarser grained than the basaltic enclaves, and plagioclase phenocrysts are not visible on fresh surfaces. In addition, their margins are more diffuse than those of the basaltic enclaves, and the granodiorite adjacent to the enclave/host contact is somewhat darker than elsewhere.

Petrography. Biotite granodiorite has medium-grained hypidiomorphic granular texture and consists of plagioclase + K-feldspar + quartz + biotite + Fe-Ti oxides. Apatite, titanite, allanite, and zircon are accessories. Inclusions of biotite, apatite,

Fe-Ti oxides, and minor amphibole (hornblende?) are common in plagioclase. Quartz and K-feldspar have interstitial and poikilitic habits. Apatite forms euhedral acicular prisms with aspect ratios of 20:1 or greater. Amphibole occurs as small rounded blebs up to 0.1 mm in diameter.

Basaltic enclaves are porphyritic and consist of plagioclase + biotite + actinolitic hornblende + Fe oxides and accessory titanite and apatite. Euhedral to subhedral plagioclase phenocrysts reach 3.0 mm in length. Hornblende and biotite are abundant groundmass phases. Aggregates of actinolitic amphibole (up to 1.0 mm in diameter) are rimmed by biotite, and probably represent relict pyroxene (e.g., Castro et al., 1990). Apatite occurs as acicular prisms; some are hollow, and aspect ratios exceeding 30:1 are common. Enclave margins adjacent to trondhjemitic zones in the host are sharp (Fig. 3C) and locally enriched in biotite.

Andesitic enclaves contain the same mineral assemblage as the host granodiorite. Long prismatic crystals of plagioclase form

radiating clusters up to 4.0 mm in diameter (Fig. 3D). Inclusions of biotite, actinolite, apatite, and Fe-Ti oxides in plagioclase are common. Large poikilitic grains of K-feldspar up to 4.0 mm in diameter enclose plagioclase, biotite, quartz, titanite, and actinolite. Quartz is also interstitial and titanite is poikilitic. Actinolite (0.01–0.30 mm in length) occurs as small stubby blebs, tabular grains, and needles.

Late-Stage Tonalitic Dikes

Field Observations. Late-stage tonalitic dikes commonly contain mingling zones of variably hybridized enclaves. The best-exposed occurrence is on the summit of Lake Mountain. Sizes of individual enclaves range from <1 cm to >20 cm in longest dimension. Enclaves are fine- to medium-grained and black to dark gray and set in a medium- to coarse-grained, dark- to medium-gray matrix that grades into the pale gray of the tonalitic host (Fig. 4A). Contacts between the matrix and enclaves are commonly diffuse, and veins of host material in the enclaves are rare. Enclaves are typically oblate with tapered ends and aspect ratios <2:1. The enclaves are crudely oriented parallel to the gradational contact between the hybrid matrix and the tonalitic dike (Fig. 4A).

Enclaves are generally isolated, separated from one another by as much as 10–15 cm of matrix. They exhibit a wide range of grain sizes, as does the matrix, thereby making it difficult to discern the outlines of smaller enclaves. In fact, the matrix is littered with small, barely recognizable enclaves, which made sampling for chemical analysis difficult (Fig. 4B).

Petrography. The biotite tonalite consists of plagioclase (An_{28-37}) + quartz + biotite + Fe oxides ± hornblende ± K-feldspar. Accessory phases are apatite, as inclusions in plagioclase, and zircon. Euhedral to subhedral plagioclase (up to 3.0 mm in length) exhibits weak normal zonation. Quartz and minor K-feldspar are interstitial. Minor hornblende occurs as inclusions in biotite.

Microdioritic enclaves consist of plagioclase (An_{45-49}) + hornblende + biotite + Fe-Ti oxides + clinopyroxene + orthopyroxene ± quartz. Apatite is common, with aspect ratios of 5:1–10:1. Enclaves commonly exhibit a strong foliation defined by the alignment of euhedral to subhedral hornblende and plagioclase. Biotite is poikilitic and quartz is interstitial. Pyroxene occurs as cores in hornblende and as large clots rimmed with hornblende.

Rocks from the dark “hybrid” matrix appear to contain components of both enclave and host, resulting in a strongly bimodal distribution of grain size (Fig. 4C). Strongly zoned plagioclase grains with resorbed rims and cores are common, although unresorbed grains are also present. Pyroxene is generally rimmed with hornblende. Apatite exhibits two habits: long, acicular needles and short, stubby prisms. Relatively siliceous hybrid compositions contain more biotite, plagioclase, and quartz, and less pyroxene and hornblende.

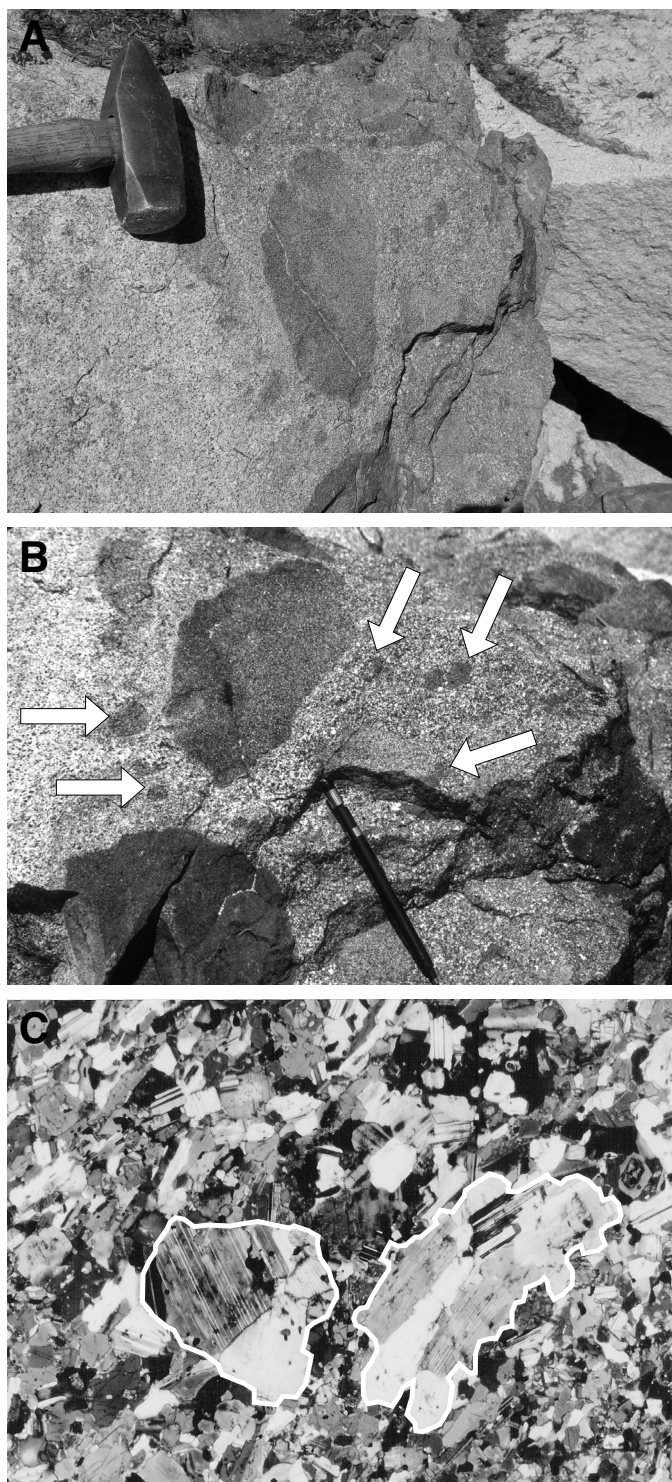


Figure 4. Photographs and photomicrographs of enclaves in late-stage tonalitic dikes. (A) Dioritic enclaves in dark colored hybrid matrix, which grades into lighter-colored tonalite (at hammer head). (B) Enclaves within hybrid matrix of the tonalitic dike. Arrows point to small, inconspicuous enclaves, which contribute to the bimodal grain size in the hybrid matrix. (C) Coarse-grained crystal aggregates (outlined) within the hybrid matrix of a tonalitic dike (field of view is 6.0 mm).

WHOLE-ROCK GEOCHEMISTRY

Mafic Enclave Swarms

Micronoritic enclaves from the Grayback Mountain enclave swarm most closely resemble high-Al island arc tholeiites, on the basis of their low K_2O and high CaO/Al_2O_3 and $FeO^*/$

MgO (Table 1, Fig. 5). There is little difference between enclave and host compositions, with the exception of slightly higher K_2O , Cr, Zr, and Rb, and slightly lower TiO_2 , Fe (total Fe as FeO), and Ni abundances in the host (Fig. 6). In addition, host material (GM-25-8) adjacent to a large enclave contains higher Na_2O , V, Nb, Y, Zr, and Ba, and lower MgO than host material isolated from enclaves (Table 1).

TABLE 1. MAJOR AND TRACE ELEMENT COMPOSITIONS OF REPRESENTATIVE SAMPLES FROM THE GRAYBACK PLUTON MAGMA MINGLING ZONES

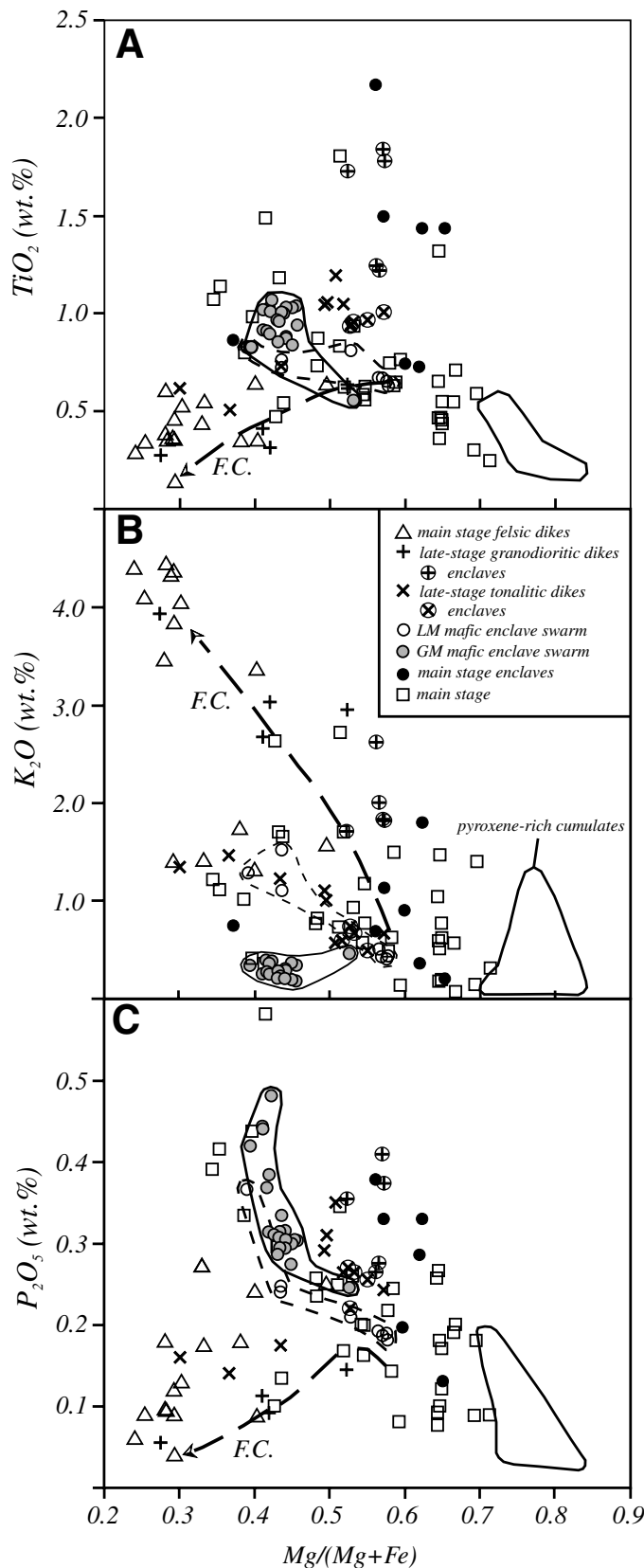
Sample	SiO ₂	TiO ₂	Al ₂ O ₃	Fe*	MnO	MgO	CaO	Na ₂ O	K ₂ O	P ₂ O ₅	LOI	Total	Sc
Mafic Enclave Swarms													
GM-2A	48.90	0.92	20.49	10.84	0.19	3.83	9.95	3.26	0.25	0.44	0.46	99.52	23.5
GM-1A	49.96	1.03	18.18	12.58	0.24	5.01	10.65	2.58	0.21	0.32	0.18	100.90	34.3
GM-1B	50.84	1.02	18.69	11.85	0.21	4.17	9.70	2.93	0.26	0.44	0.67	100.78	25.4
GM-24	50.08	0.55	19.26	9.05	0.17	5.09	12.01	2.27	0.45	0.25	1.24	100.41	38.0
GM-25-1	48.06	0.94	18.82	12.42	0.21	5.26	10.27	2.69	0.35	0.30	0.58	99.89	43.5
GM-25-2	48.99	0.89	18.51	12.71	0.22	5.07	10.06	2.57	0.31	0.30	0.61	100.23	36.1
GM-25-3	49.34	0.88	18.61	12.60	0.23	5.03	10.37	2.33	0.28	0.30	0.63	100.59	35.8
GM-25-4	49.26	0.87	18.30	12.84	0.23	5.13	10.42	2.36	0.29	0.30	0.60	100.59	35.7
GM-25-5	49.77	0.86	18.32	12.90	0.23	4.94	10.11	2.30	0.29	0.31	0.68	100.70	34.4
GM-25-6	48.25	0.84	18.60	12.51	0.23	5.16	11.17	2.40	0.37	0.27	0.58	100.38	39.9
GM-25-7	48.55	0.90	18.65	14.08	0.24	5.13	9.65	2.32	0.29	0.31	0.61	100.72	38.0
GM-25-8	49.97	0.91	19.66	10.56	0.15	3.80	9.86	3.19	0.40	0.37	0.73	99.60	38.4
LM-11	53.23	0.82	18.65	10.50	0.21	3.41	8.70	3.10	1.28	0.37	n.d.	100.27	n.d.
LM-7-1	57.04	0.73	19.36	6.63	0.09	2.59	7.39	3.03	1.10	0.25	1.92	100.12	4.8
LM-7-2	52.07	0.67	14.61	11.13	0.22	7.44	10.71	1.94	0.43	0.19	0.53	99.94	49.1
LM-7-3	52.23	0.65	15.49	10.46	0.21	7.16	10.83	2.06	0.41	0.19	0.42	100.11	43.2
LM-7-4	52.52	0.63	15.43	10.11	0.21	6.99	11.13	2.30	0.43	0.18	0.45	100.38	45.3
LM-7-5	52.08	0.67	15.42	10.60	0.21	6.96	10.61	2.33	0.50	0.19	0.51	100.08	50.0
LM-7-6	50.25	0.81	15.87	11.62	0.23	6.56	10.23	2.38	0.67	0.21	0.58	99.41	50.0
LM-7-7	57.67	0.76	18.71	6.59	0.08	2.57	6.73	2.70	1.52	0.24	1.58	99.15	4.8
Late-stage granodioritic dikes													
LM-1	54.85	1.73	17.27	8.03	0.17	4.45	7.60	3.91	1.71	0.36	1.11	101.18	22.6
LM-2	73.75	0.27	13.81	2.68	0.07	0.51	1.76	3.16	3.94	0.06	0.60	100.61	n.d.
LM-3	73.03	0.32	14.52	2.11	0.04	0.77	2.29	3.71	3.03	0.09	0.69	100.60	4.0
LM-18A	51.69	1.84	17.68	8.90	0.17	5.96	7.85	3.68	1.83	0.41	0.87	100.88	23.5
LM-18B	71.07	0.41	14.64	2.87	0.05	1.01	2.46	3.86	2.67	0.11	0.73	99.89	5.6
LM-29A	51.35	1.78	17.37	8.61	0.15	5.82	8.06	3.71	1.82	0.37	1.01	100.05	23.3
LM-29B	69.14	0.62	14.56	3.51	0.06	1.94	3.08	3.76	2.96	0.15	0.91	100.68	8.1
LM-29C	59.56	1.25	15.60	6.39	0.12	4.14	5.42	3.74	2.62	0.27	0.77	99.87	15.8
LM-29D	59.68	1.22	15.67	6.32	0.11	4.15	5.63	3.99	2.00	0.25	0.90	99.95	15.4
GBP-152B	71.99	0.36	14.88	2.30	0.04	0.78	2.41	3.67	3.36	0.09	0.00	99.88	4.5
Late-stage tonalitic dikes													
LM-15A	47.97	1.01	15.19	12.29	0.25	8.32	11.46	1.44	0.66	0.24	1.25	100.08	58.3
LM-16B	51.21	0.96	16.21	10.90	0.19	6.25	9.68	3.26	0.68	0.27	0.67	100.28	44.0
LM-16C	50.08	0.97	16.02	11.11	0.19	6.88	10.68	2.80	0.49	0.26	0.46	99.94	46.9
LM-19	50.88	1.20	17.29	10.67	0.21	5.57	9.76	3.06	0.57	0.35	0.54	100.10	40.3
LM-26A1	52.47	0.95	15.66	10.73	0.20	6.05	9.20	3.24	0.75	0.22	0.67	100.14	43.1
LM-26A2	54.48	1.05	17.35	9.40	0.18	4.62	8.16	3.28	1.11	0.29	0.90	100.82	35.2
LM-26A3	63.35	0.73	16.72	5.99	0.13	2.32	4.97	3.60	1.23	0.18	0.86	100.08	15.5
LM-27A	54.15	1.06	17.31	9.64	0.19	4.80	8.33	3.17	1.00	0.31	1.31	101.28	33.6
LM-27B2	50.70	1.05	16.80	11.41	0.21	6.19	10.02	3.12	0.59	0.27	0.50	100.86	46.3
LM-28	67.65	0.51	16.04	4.17	0.08	1.22	4.07	4.06	1.47	0.14	0.62	100.02	8.2
LM-10	62.88	0.62	17.68	5.50	0.09	1.19	4.41	4.58	1.35	0.16	n.d.	98.46	9.9

Notes: Major element oxides are expressed in wt%; trace elements in ppm. Total Fe as Fe_2O_3 . Samples starting with "GM" are from Grayback Mountain; those beginning with "LM" are from Lake Mountain. Abbreviation: n.d.—not determined.

Unlike enclave-host relationships exposed on Grayback Mountain, enclaves in the Lake Mountain enclave swarm are more chemically distinct from their host (Table 1, Fig. 6). Lake Mountain enclaves have lower SiO₂, TiO₂, Al₂O₃, Na₂O, K₂O, P₂O₅, Zr, Sr, Ba, Rb, and FeO*/MgO, and higher MgO, CaO, Sc, V, Cr, Ni, Y, and CaO/Al₂O₃ than their host rocks (Fig. 6). Enclave compositions are similar to calc-alkaline basalt and

basaltic andesite on the basis of their higher K₂O and lower FeO*/MgO, relative to tholeiitic compositions. Enclave and host samples have light REE (LREE)-enriched chondrite-normalized patterns (Fig. 7). The host sample (LM-11) has a straight REE pattern, whereas the enclave (LM-7-4) has higher Σ REE and exhibits a negative Eu anomaly (Eu/Eu* = 0.73). Both enclave and host have similar initial ⁸⁷Sr/⁸⁶Sr (0.7042) and

V	Cr	Ni	Cu	Zn	Nb	Y	Zr	Ba	Sr	Rb	Rock
228	27	11	91	92	16	19.7	22	248	620	3	Enclave
293	8	12	55	111	24	13.6	10	219	513	2	Enclave
247	37	10	90	107	19	19.9	22	225	575	4	Enclave
223	77	24	283	75	16	17.5	58	259	497	7	Host
279	12	8	117	102	23	29.7	37	251	482	3	Enclave margin
290	12	12	109	112	23	20.2	21	232	480	3	Enclave-core
292	10	13	172	119	26	19.9	21	226	483	3	Enclave-core
282	28	115	164	109	26	20.2	30	226	480	3	Enclave-core
293	9	10	191	108	23	19.2	40	226	482	3	Enclave-core
294	11	10	135	117	27	23.8	19	232	487	3	Enclave-core
300	16	36	111	130	28	24.6	15	225	492	3	Enclave margin
268	30	14	125	89	22	31.1	73	317	542	5	Host adjacent to enclosure
n.d.	n.d.	n.d.	n.d.	n.d.	n.d.	28.8	17	546	475	33	Host
174	27	10	119	66	12	4.6	107	602	470	24	Host adjacent to enclosure
257	140	32	98	100	24	36.9	43	177	304	5	Enclave margin
241	127	30	130	86	20	31.2	55	176	315	4	Enclave-core
224	124	29	136	87	19	33.5	62	174	325	4	Enclave-core
222	111	26	152	92	19	35.4	57	197	334	6	Enclave-core
223	96	28	86	93	18	35.6	40	284	340	9	Enclave margin
122	29	14	54	60	7	4.3	151	1131	470	38	Host adjacent to enclosure
170	112	47	28	83	33	37.3	169	218	339	62	Enclave-basalt
n.d.	n.d.	n.d.	n.d.	n.d.	n.d.	n.d.	n.d.	1342	154	75	Host
24	12	5	4	33	5	10.3	141	970	241	63	Host
184	156	83	26	74	24	28.6	172	184	355	62	Enclave-basalt
32	18	11	20	73	24	27.2	154	189	371	55	Enclave-basalt
174	158	86	6	32	12	21.3	133	774	292	48	Host
57	47	31	6	57	18	27.0	135	457	282	55	Enclave-andesite
122	114	75	7	56	19	23.2	150	320	284	45	Enclave-andesite
25	10	7	5	39	19	15.0	155	1108	235	50	Host
305	135	11	43	122	1	31.0	50	239	395	15	Enclave
243	98	7	35	113	2	29.0	64	323	399	11	Enclave
259	119	10	113	118	2	28.3	49	226	429	7	Enclave
225	64	4	19	119	4	28.9	73	243	501	10	Enclave
225	107	6	24	121	4	28.7	56	361	390	15	Enclave
188	45	3	17	101	4	28.5	112	521	453	29	Matrix
88	18	4	8	73	3	7.9	189	769	432	39	Host
193	49	6	17	108	3	24.0	87	505	468	26	Matrix
237	79	15	12	111	5	40.0	28	269	435	10	Enclave
53	9	4	4	49	3	10.7	229	1088	366	59	Host
51	8	6	7	66	11	13.4	282	895	366	31	Host



ϵ_{Nd} (+5.5 and +4.8, respectively; Barnes et al., 1995), which are comparable to rocks of the main stage of the Grayback pluton.

Late-Stage Granodioritic Dikes

Basaltic enclaves in the late-stage granodioritic dikes are high-Al and calc-alkaline in composition. They have similar SiO₂ contents to micronoritic enclaves in the mafic enclave swarms, but have higher TiO₂, Na₂O, K₂O, Zr, and Rb, and lower FeO, MnO, CaO, Sc, V, and CaO/Al₂O₃ (Table 1, Fig. 5). One enclave sample is characterized by a linear chondrite-normalized REE pattern that lacks a Eu anomaly, by high ϵ_{Nd} (+5.5), and by low initial ⁸⁷Sr/⁸⁶Sr (0.7027; Barnes et al., 1995). Apparently unmodified host granodiorite has SiO₂ >70 wt%, K₂O to nearly 4 wt%, and Ba abundances of 800–1342 ppm (Fig. 5). In addition, a granodiorite sample has low heavy REE (HREE) abundances (Yb_N = 5.5), and a slight negative Eu anomaly (Eu/Eu* = 0.76; Fig. 7). Andesitic enclaves are compositionally intermediate between basaltic enclaves and granodioritic host samples (Table 1); indeed, andesitic samples plot along a straight line between the basaltic and granodioritic end-members for most elements (Fig. 8).

Additional samples from the margin of an andesitic enclave and from dark-colored host granodiorite adjacent to the enclave were analyzed (Table 1). Compared to unmodified granodiorite, the granodiorite adjacent to the enclave is higher in TiO₂, FeO, MgO, CaO, Sc, V, Cr, Ni, and Y, and lower in SiO₂ and Sr. The sample from the margin of the andesitic enclave is depleted in Na₂O and Zr, but enriched in K₂O, Y, Ba, and Rb, relative to the enclave core.

Late-Stage Tonalitic Dikes

Tonalitic rocks from late-stage dikes are distinct from the main-stage tonalites. Barnes et al. (1995) characterized the late-stage rocks as high-Al tonalites, whereas main-stage tonalites are low-Al (c.f. Barker, 1979). In addition to its higher Al₂O₃ contents, the late-stage tonalite is characterized by higher SiO₂, FeO*/MgO, and Zr, and chondrite-normalized REE patterns that show greater fractionation of HREE from LREE and positive Eu anomalies.

Microdiioritic enclaves in the late-stage tonalitic dikes have similar SiO₂ contents to basaltic enclaves in the late-stage granodioritic dikes, but have higher FeO, MgO, CaO, Sc, V, Zn, Ba,

Figure 5. Variation diagrams showing compositions from the main-stage, mafic enclave swarms, and late-stage tonalitic and granodioritic dikes, including enclave and hybrid compositions. Samples within the field outlined by the solid line are from the Grayback Mountain mafic enclave swarm, whereas those within the field outlined by the dashed line represent the Lake Mountain mafic enclave swarm. Thick dashed line labeled "F.C." represents the evolution of mafic magmas by fractional crystallization (see Barnes et al., 1995). Outlined fields at Mg/(Mg + Fe) >0.7 represent the compositions of pyroxene-rich cumulates.

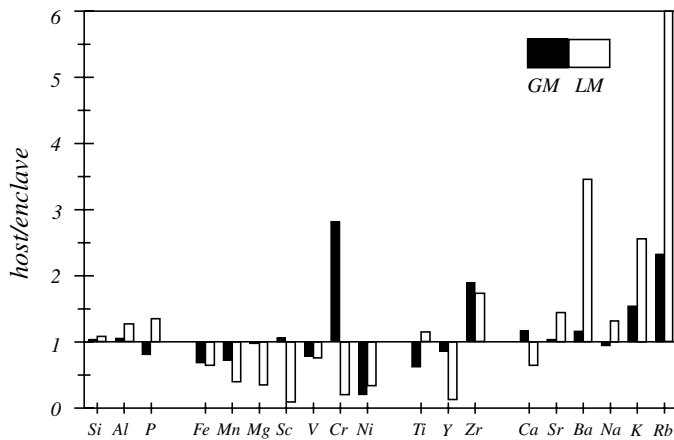


Figure 6. Enrichment-depletion diagram comparing representative enclave and host compositions from the mafic enclave swarms on Grayback (GM) and Lake (LM) Mountains. Analyses are from cores of large (9–12 cm thick) enclaves and from host rock material not directly adjacent to enclaves.

Sr, and $\text{CaO}/\text{Al}_2\text{O}_3$, and lower TiO_2 , Al_2O_3 , Na_2O , K_2O , P_2O_5 , Nb, Zr, and Rb (Table 1, Figs. 5 and 8). Concentrations of most elements in these microdioritic enclaves are similar to or intermediate between micronoritic and microgabbroic enclaves in the mafic enclave swarms, but microdiorite has higher TiO_2 , Na_2O , K_2O , Ba, and Rb, and lower CaO, Ni, and Nb. A microdioritic enclave from a late-stage tonalitic dike has a LREE-

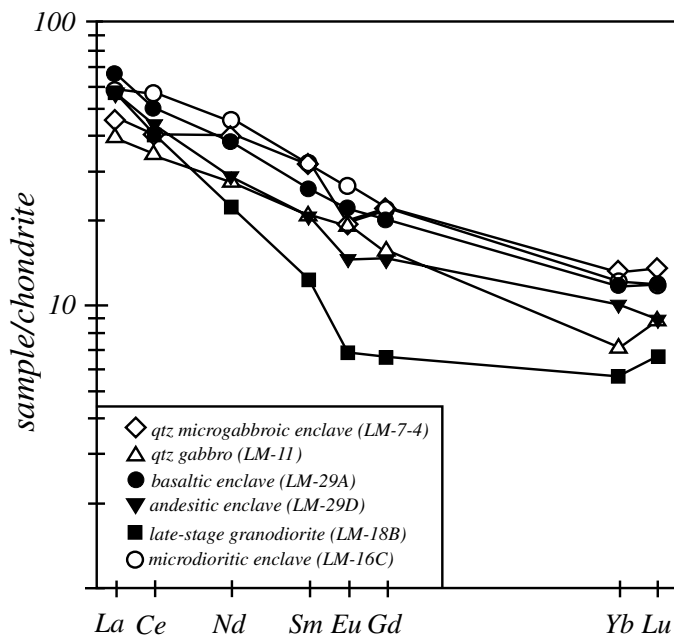


Figure 7. Chondrite-normalized rare earth element diagrams for selected samples from magma-mingling zones within the Grayback pluton. Chondrite values are from Haskin et al. (1968). Samples LM-18B, LM-29A, and LM-29D are from the same granodioritic dike.

enriched chondrite-normalized pattern, and lacks a Eu anomaly ($\text{Eu}/\text{Eu}^* = 0.99$; Fig. 7). This same enclave yielded an initial $^{87}\text{Sr}/^{86}\text{Sr}$ value similar to those of a microgabbroic enclave and its host from the mafic enclave swarm on Lake Mountain (0.7042), but has a much higher ϵ_{Nd} (+10.3; Barnes et al., 1995).

The dark matrix that envelops enclaves in the late-stage tonalitic dikes has a wide range of compositions, from ~51 to 63 wt% SiO_2 (Table 1). There is considerable overlap of matrix compositions and those of enclave and tonalitic samples, which reflects the difficulty in distinguishing the different lithologies (e.g., micro-enclaves in similarly dark matrix rock; Fig. 4B). Matrix compositions plot along straight lines between enclave and tonalitic end-members for most elements, with the marked exception of TiO_2 and P_2O_5 , which are generally higher in matrix compositions (Fig. 8).

INTERACTIONS BETWEEN MAGMAS IN THE MINGLING ZONES

Enclaves in the Grayback pluton mingling zones possess characteristics that indicate they were liquid or only partially crystallized when brought into contact with their host magmas. For example, their fine grain size, evidence for plastic deformation, and the acicular nature of apatite crystals preclude an autolithitic (e.g., early cumulate) origin and suggest that the enclave magmas were undercooled by contact with the host magma. Below, we discuss the nature of the interactions between magmas in the various magma-mingling zones exposed in the Grayback pluton and the implications of these mingling zones for magma mixing processes in the petrogenesis of the Grayback system.

Mafic Enclave Swarms

The mafic enclave swarms on Grayback and Lake Mountains represent relatively early mingling episodes in the Grayback pluton. Moreover, they represent mingling between two or more mafic and/or intermediate magmas, as opposed to mingling between mafic and felsic compositions, as in the late-stage dikes. The mingling zone on Grayback Mountain is unusual in that there is little compositional difference between enclave and host rocks.

One of the puzzling features of the mafic enclave swarms is the aggregates of coarse-grained poikilitic hornblende and plagioclase within finer-grained pyroxene-rich enclaves (Fig. 2C and F). We interpret these as relict veins of host material caught between enclaves during emplacement. The residual liquid in the veins was either squeezed out or incorporated into the enclave magma during localized contraction. In this scenario, the coarser hornblende and plagioclase would be xenocrystic to the enclaves, akin to the quartz ocelli frequently described in mafic enclaves in quartz-rich host rocks (e.g., Vernon, 1983). The preservation of quartz ocelli in mafic enclaves is typically cited as evidence that the enclaves represent hybrid compositions, which is taken to imply that magma mixing occurred prior to commingling and enclave formation.

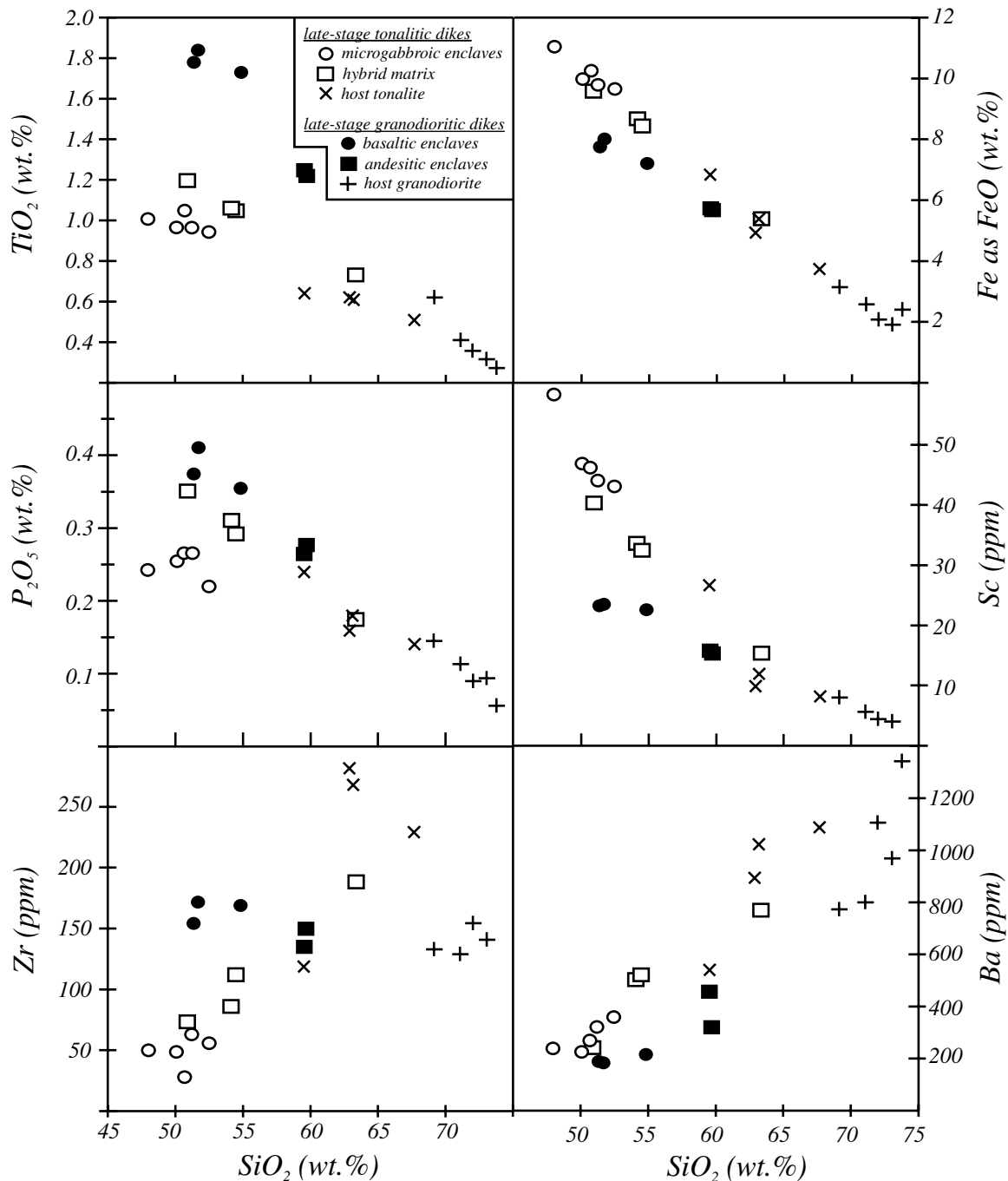


Figure 8. Harker diagrams of selected elements vs. SiO_2 for mafic enclave, felsic host, and intermediate hybrid compositions in the late-stage granodioritic and tonalitic dikes.

Some veins of the host rock contain fragments of enclave material that were apparently separated from the enclave during vein formation. Thus, field evidence indicates that hybridization of the magmas occurred in two ways: (1) incorporation of host magma into enclave magma by collapse of veins, and (2) fragmentation of enclave material into the host magma. This mechanism of hybridization might explain why there is less

compositional distinction between enclave and host rocks on Grayback Mountain, where the degree of localized flattening and thus incorporation of host magma into the enclaves, was apparently greater than on Lake Mountain.

It could be argued that enclave and host rocks in the Lake Mountain mingling zone represent the mafic and more evolved components, respectively, of a single magma undergoing frac-

tional crystallization. However, the host has higher TiO_2 , Al_2O_3 , P_2O_5 , Sr, and Zr, and lower ΣREE than the enclaves, which is not the expected result of fractional crystallization of the observed phases. Therefore, we conclude that enclave and host compositions in the Lake Mountain mafic enclave swarm represent magmas from two calc-alkaline sources.

Although their outcrops are similar in appearance, it is clear that rocks comprising the mafic enclave swarm on Grayback Mountain are very different in composition from those exposed on Lake Mountain (Fig. 5). In contrast to Grayback Mountain samples, those from the Lake Mountain mafic enclave swarm are similar in composition to rocks comprising the noncumulate main stage of the Grayback pluton.

Late-Stage Granodioritic Dikes

The presence of both basaltic and andesitic enclaves in the late-stage granodioritic dikes suggests either that the enclave magmas were derived from two distinct sources or that the andesitic enclaves represent a hybridized mixture of basaltic and granodioritic magmas. We tested the mixing scenario, using element ratios according to the method of Langmuir et al. (1978). If a suite of rocks is related by binary mixing, then the samples should define a hyperbolic curve in ratio-ratio plots, define straight lines in companion plots, and remain in the same relative order in both ratio-ratio and companion plots. This approach, using Sc, Cr, K, and Ba abundances (Fig. 9A), produced consistent results that suggest binary mixing of basaltic and granodioritic end-members formed the andesitic magma. Major element least-squares mass balance calculations indicate that a mixture of 58% basalt and 42% granodiorite would produce a hybrid composition similar to that of the andesite (Table 2). Mixing calculations using the REE abundances of the same basaltic and granodioritic end-members produced hybrid compositions with chondrite-normalized REE patterns similar to the andesitic enclaves (Fig. 9B).

The presence of basaltic and hybrid andesitic enclaves in the late-stage granodioritic dikes is suggestive of a multi-stage mixing/mingling process (Koyaguchi, 1986). In the first stage, basaltic magma intruded the silicic magma, producing a layer of hybrid andesite at their interface. In the second stage, dike formation and magma ascent disrupted the basaltic and andesitic layers, resulting in their incorporation as enclaves in the silicic host magma. A post-emplacment stage involved chemical exchange between the magmas. The abundance of biotite and actinolite in the basaltic enclaves and the biotite- and K-feldspar-poor trondhjemitic halo that envelops several enclaves is suggestive of migration of H_2O and K^+ from the granodioritic to basaltic magmas (Watson and Jurewicz, 1984).

Major element mass balance calculations indicate that the dark-colored granodioritic host adjacent to some andesitic enclaves represents a mixture of ~18% andesitic and 82% granodioritic magmas (Table 2). The andesitic magma would have had a lower temperature and a resultant higher viscosity, relative to the basaltic magma, which would have prevented com-

plete mechanical mixing of the andesitic and granodioritic magmas. We suggest instead that the dark-colored granodiorite formed by late-stage diffusive exchange between andesitic and granodioritic magmas during and/or after emplacement of the dike. This post-emplacment exchange was more pronounced than that between basaltic enclaves and host, because the basaltic magma was supercooled to a greater degree, which would have hindered chemical diffusion.

Late-Stage Tonalitic Dikes

As in the case of the late-stage granodioritic dikes, ratio-ratio and companion diagrams using enclave, host, and intermediate samples from late-stage tonalitic dikes (in this case, using Sc, Cr, Zr, and Ba abundances) suggest that magma mixing played a dominant role in the formation of intermediate compositions (Fig. 10). Minor deviations from linearity in the companion diagrams may result from fractional crystallization of augite in the enclave magma (see also Smith et al., 1990; Wiebe et al., 2002), resulting in enclave compositions with lower Sc/Zr values than those predicted for mixing alone (Fig. 10).

Major element mass-balance calculations suggest that binary mixing between dioritic and tonalitic magmas can produce almost the entire range of intermediate compositions observed in the late-stage tonalitic dikes. Most calculations yielded acceptable results (sum of the squares of residuals [Σr^2]) less than unity; Table 2). However, high negative Al_2O_3 residuals and high positive MgO and CaO residuals in some calculations (Table 2) suggest accumulation of plagioclase in, and possibly removal of augite from, the hybrid magma.

Anomalously high TiO_2 and P_2O_5 abundances in hybrid rocks have been noted in mingling zones elsewhere (Wood, 1978; Vogel, 1982; Marshall and Sparks, 1984; D'Lemos, 1996; Kuritani et al., 2003) and have been attributed to pre-mixing fractional crystallization in the mafic magma, mixing between compositionally heterogeneous magmas, post-mixing TiO_2 and P_2O_5 enrichment in the hybrid, and anomalous diffusion of Ti and P complexes. Enrichment of TiO_2 in the matrix compositions is inconsistent with the removal of augite from the hybrid magma (see above), and mixing between heterogeneous magmas is not suggested by the uniform TiO_2 and P_2O_5 in enclave and host samples. Alternatively, nonlinear relationships might reflect differences in diffusion coefficients between the elements of interest. However, differences in diffusion coefficients are unlikely to affect element correlations at the scale of hand samples used in this study (Perugini and Poli, 2004). In light of the fractional crystallization scenario described above, we suggest that the anomalously high TiO_2 and P_2O_5 contents in the matrix samples (Fig. 8) are a reflection of pre-mixing removal of augite (and apatite) from the enclave magma.

Discussion of Rheologic Models

Introduction. Petrographic observations and whole-rock chemical compositions can be used to estimate the rheologic

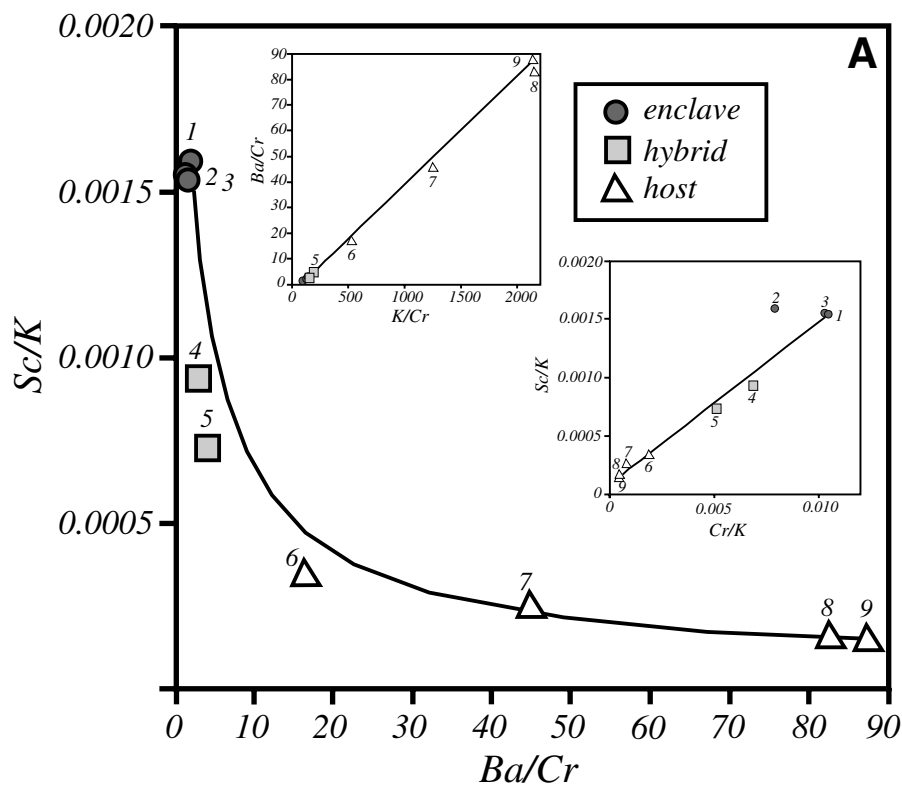


Figure 9. (A) Ratio-ratio and companion (insets) diagrams for basaltic and andesitic enclave and host compositions from a late-stage granodioritic dike. The solid lines represent the calculated hybrid compositions produced by mixing of basaltic and granodioritic magmas. The numbered samples in the diagram of Sc/K vs. Ba/Cr generally retain their relative order in the companion diagrams, suggesting that the intermediate compositions are hybrids of the two end-members (Langmuir et al., 1978). (B) Chondrite-normalized rare-earth element diagram comparing the composition of an andesitic enclave (LM-29D) with the calculated mixture (dashed line) of 58% basaltic enclave (LM-29A) and 42% granodioritic host (LM-18B) magmas, as suggested by major element mass-balance calculations.

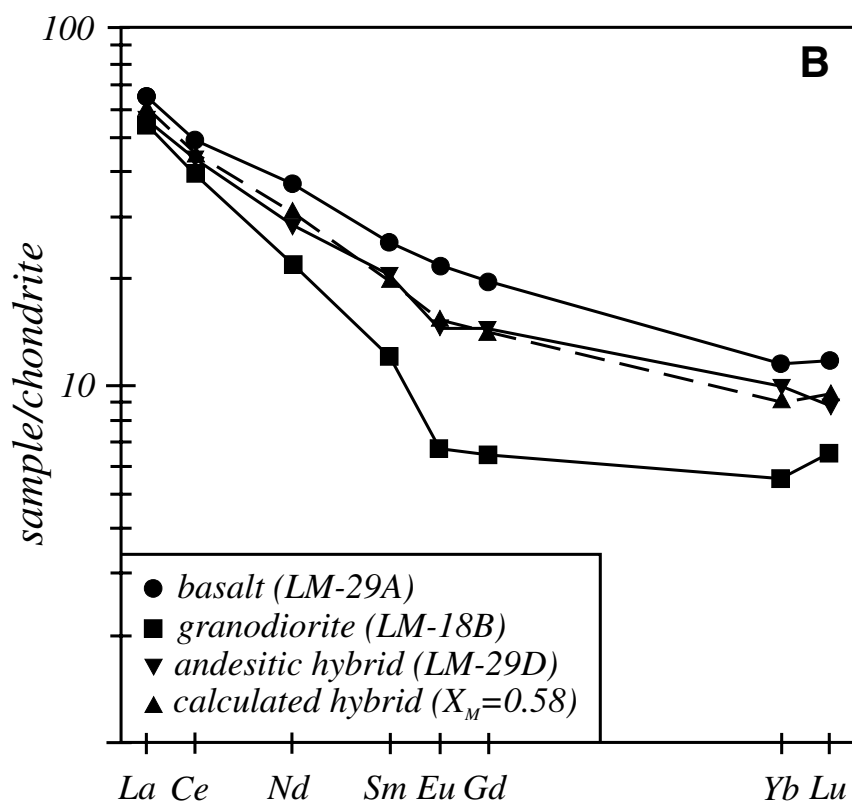


TABLE 2. RESULTS OF MAJOR ELEMENT MIXING CALCULATIONS FOR SAMPLES FROM THE LATE-STAGE GRANODIORITIC AND TONALITIC DIKES

Model	Mafic	Residuals										Felsic	Mix	X_M	ssr
		SiO ₂	TiO ₂	Al ₂ O ₃	FeO	MnO	MgO	CaO	Na ₂ O	K ₂ O	P ₂ O ₅				
1A	LM-29A	-0.05	-0.01	0.55	-0.11	-0.00	-0.35	0.08	-0.22	0.18	-0.01	LM-18B	LM-29D	0.58	0.53
1B	LM-29D	-0.10	-0.07	0.26	-0.02	0.01	-0.37	-0.06	0.12	-0.41	-0.00	LM-18B	LM-29B	0.18	0.41
2A	LM-27B2	0.22	-0.09	-0.50	-0.07	-0.03	0.10	0.53	0.23	0.03	-0.00	LM-28	LM-26A3	0.24	0.66
2B	LM-16C	0.22	-0.12	-0.68	-0.19	-0.03	0.21	0.63	0.17	0.01	-0.01	LM-28	LM-26A3	0.23	1.05
2C	LM-27B2	0.30	-0.13	-0.73	0.24	0.00	0.37	0.43	0.07	-0.31	-0.06	LM-28	LM-26A2	0.76	1.13
2D	LM-16C	0.19	-0.03	-0.19	-0.28	-0.00	0.21	0.50	-0.37	-0.12	-0.02	LM-28	LM-16B	0.93	0.59

Notes: The terms "Mafic," "Felsic," and "Mix" refer to the mafic, felsic, and observed hybrid compositions, respectively, used in the calculations. Residuals are the differences between the calculated mixture and the observed mixture. Abbreviations: X_M —proportion of mafic and member used in the calculations; ssr—sum of the squares of the residuals.

conditions under which magma mixing and mingling are possible (Sparks and Marshall, 1986; Frost and Mahood, 1987). Complete mixing between two magmas of contrasting compositions requires the equilibrium temperature of the mixture to be greater than the solidus temperature of the mafic end-member. The equilibrium temperature depends on the initial temperatures and mass fractions of the end-member magmas, the heat capacities of liquid and solid components, and the heats of fusion of the solids (Frost and Mahood, 1987).

Viscosity (η)-composition relationships from the mingling zones in the Grayback pluton were determined using the algo-

rithms compiled by Frost and Lindsay (1988). Resultant viscosity curves are shown in Figures 11–14, with respect to the mass fraction of the mafic end member in each mixture (X_M). Intersections of viscosity curves of coexisting magmas are circled, and represent the conditions at which both magmas possess equal viscosities (η^* , the "equilibrium" viscosity), and are thus most likely to mix. However, it should be noted that hybridization can occur between magmas with viscosity differences as great as 10^2 poise (Frost and Mahood, 1987) and at X_M greater than that at η^* (Sparks and Marshall, 1986). Terminations of the mafic end-member curves represent the η and X_M values where

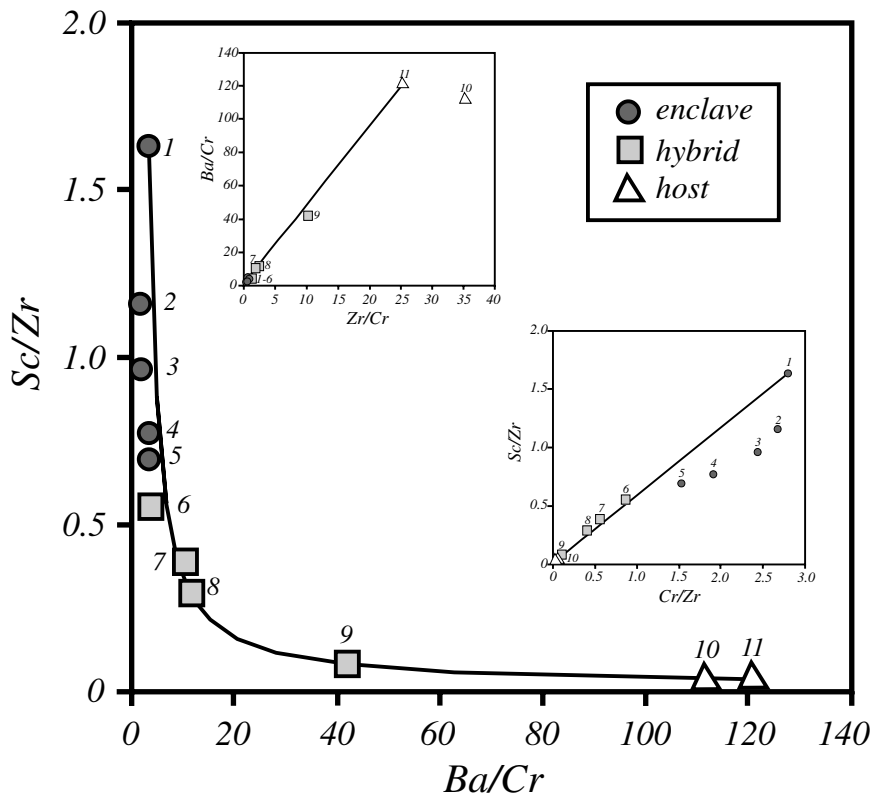


Figure 10. Ratio-ratio and companion (insets) diagrams for microdioritic enclave, hybrid matrix, and host tonalite compositions in a late-stage tonalitic dike. The solid lines represent the calculated hybrid dike compositions produced by mixing of dioritic and tonalitic magmas. As in Figure 9, the numbered samples in the ratio-ratio diagram generally retain their relative order in the accompanying companion diagrams, suggesting a mixing origin for intermediate compositions. Deviation of hybrid compositions from the calculated mixing line in the companion plot of Sc/Zr vs. Cr/Zr probably reflects fractional crystallization of augite (see text).

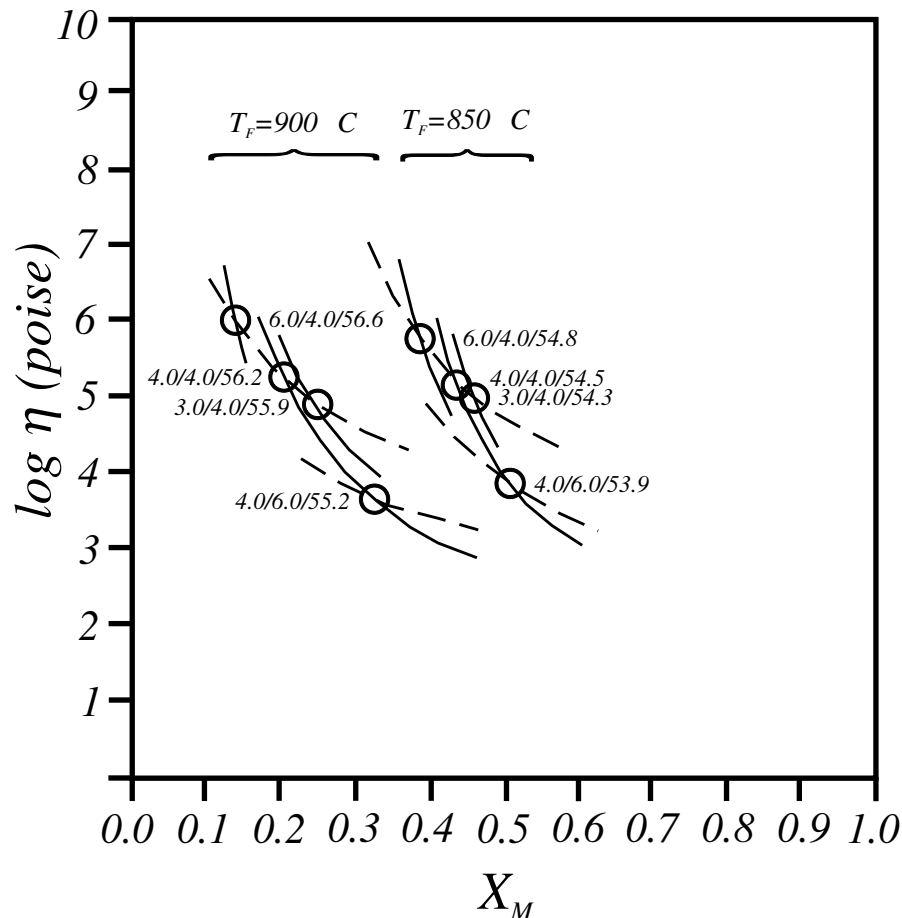


Figure 11. Viscosity-composition diagram for enclave-host pairs in the Lake Mountain mafic enclave swarm, showing the variations in viscosity and composition of hybrid magmas as a function of initial temperatures and H_2O contents of the enclave (solid curves) and host (dashed curves) magmas. Only the intersections of enclave-host pairs are shown and are labeled X/Y/Z, where X is the initial H_2O content of the enclave magma, Y is the initial H_2O content of the host magma, and Z is the SiO_2 content (in wt%) of the resultant hybrid. Two sets of intersections are shown for initial host magma temperatures of 850 °C and 900 °C.

the mafic magma is >60% crystallized, and thus essentially acts as a solid (Frost and Mahood, 1987).

Lake Mountain Mafic Enclave Swarm. One of the puzzling aspects of the mafic enclave swarms is the preservation of enclave and host, despite their compositional similarities. If these rocks are reflective of magma mingling in the main stage of the pluton, then it can be assumed that main-stage mixing occurred earlier in the Grayback system and that conditions changed enough to prohibit thorough mixing of these magmas within the enclave swarm. The rheological properties of enclave and host compositions were investigated in an effort to determine why the magmas did not mechanically mix within the mafic enclave swarm at the present level of exposure.

The hornblende-rich nature of enclaves and host rocks in the Lake Mountain enclave swarm suggests that both enclave and host magmas had initial H_2O contents >3.0 wt% (e.g., Sisson and Grove, 1993). For an enclave magma temperature of 1050 °C, mixing to produce an intersection of mafic and felsic curves at $\dot{\eta}$ requires a host magma temperature <950 °C. Temperatures >950 °C result in enclave magma with a lower viscosity than the host magma at all values of X_M . A relatively small decrease in host magma temperature (50 °C) results in a

large increase in X_M ($\Delta X_M > 0.2$) required for mixing at $\dot{\eta}$ (Fig. 11). For mixing at equal viscosities, an increase in enclave magma H_2O content results in a slight increase in $\dot{\eta}$ and a slight decrease in X_M (Fig. 11), whereas increasing the host magma H_2O content results in slightly decreasing $\dot{\eta}$ and increasing X_M .

Complete mixing between the enclave and host magmas would have required at least 15% of the enclave end-member. That complete mixing did not occur within the mafic enclave swarm may reflect a mass decrease in the enclave end member to below 15%, or a shift of $\dot{\eta}$ to higher values of X_M as a result of lower magma temperatures or loss of H_2O from the enclave magma (Fig. 11).

Late-Stage Granodioritic Dikes. Figure 12 shows viscosity-composition curves that describe mixing between basaltic and granodioritic magmas from the late-stage granodioritic dikes. The presence of plagioclase phenocrysts and the lack of early hornblende suggest that the basaltic magma had less than ~3.0 wt% H_2O (e.g., Eggler, 1972). Rare hornblende inclusions in plagioclase and the lack of evidence for vapor saturation constrain the H_2O content in the granodioritic magma to between ~4.0 and 6.5 wt% (Naney, 1983). Mixing of anhydrous basaltic magma with granodioritic magma having 4.0 wt% H_2O would

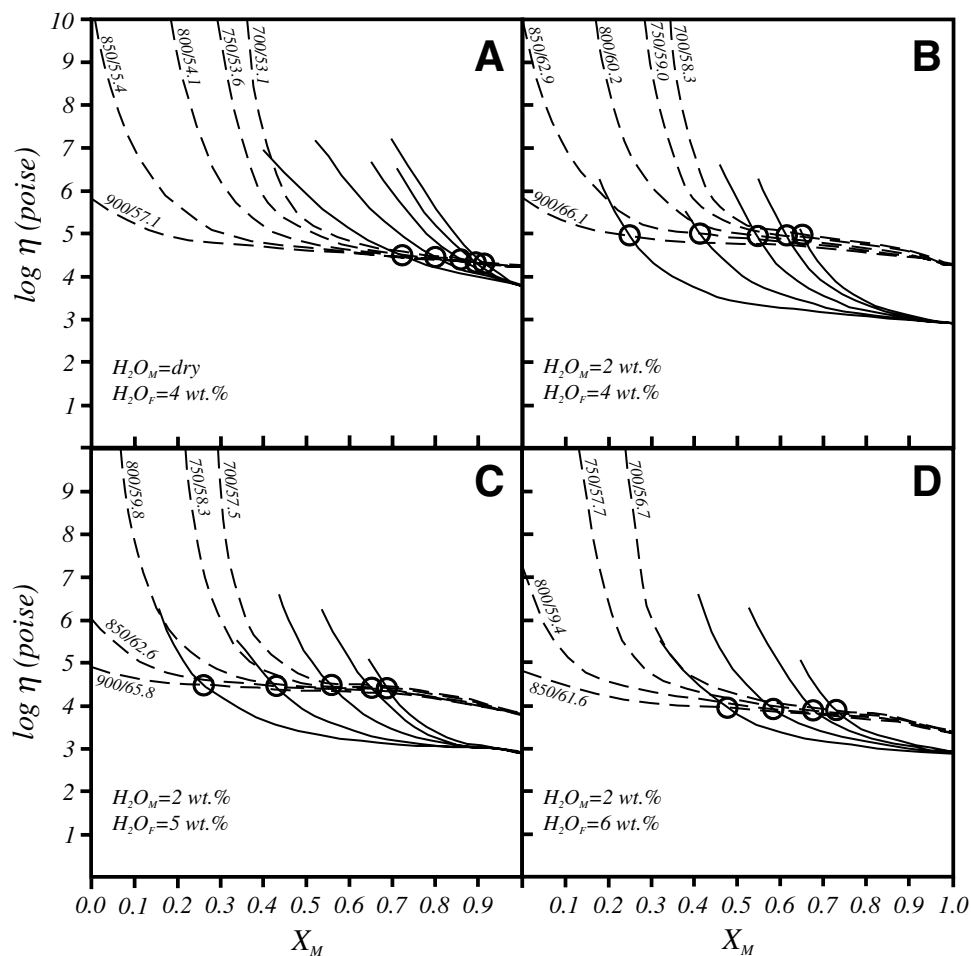
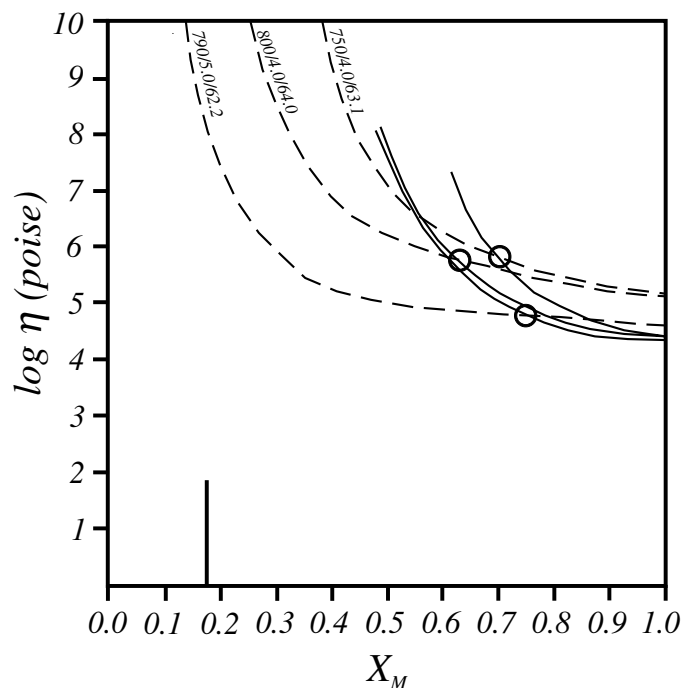


Figure 12. Viscosity-composition diagram for enclaves (basalt)-host pairs in a late-stage granodioritic dike, showing the variations in viscosity and composition of hybrid magmas as a function of initial temperatures and H_2O contents of the enclaves (solid curves) and host (dashed curves) magmas. Each panel in the figure represents different conditions of initial H_2O contents in the enclaves (H_2O_M) and host (H_2O_F) magmas. The dashed curves in each panel are labeled X/Y, where X is the initial temperature (in $^{\circ}C$) of the host magma and Y is the SiO_2 content (in wt%) of the resultant hybrid.



result in a relatively narrow range of hybrid compositions (~ 53 – 57 wt% SiO_2), requiring $X_M > 0.7$ (Fig. 12A). In contrast, mixing involving hydrous basaltic magma (2.0 wt% H_2O) results in a wider spectrum of hybrid compositions (~ 56 – 66 wt% SiO_2) requiring proportionally less mafic magma ($X_M = 0.25$ – 0.73 ; Fig. 12B–D), depending on the initial temperature and H_2O content of the host magma. The equilibrium viscosity η decreases from 10^5 to 10^4 poise with increasing H_2O content in the host magma (Fig. 12B–D). At $X_M = 0.58$, the proportion of enclaves magma estimated by major and trace element mass

Figure 13. Viscosity-composition diagram for enclaves (andesite)-host pairs in the same late-stage granodiorite (as in Fig. 12), showing variations in viscosity and composition of the hybrid, which is assumed to be the dark-colored granodiorite adjacent to several andesitic enclaves, as a function of initial temperatures and H_2O contents of the enclaves (solid curves) and host (dashed curves) magmas. Dashed curves are labeled X/Y/Z, where X is the initial temperature of the host magma, Y is the initial H_2O content of the host magma, and Z is the SiO_2 content (in wt%) of the resultant hybrid. The vertical line at $X_M = 0.18$ represents the proportion of enclaves magma required by major element mass balance to produce the dark-colored granodiorite (see text).

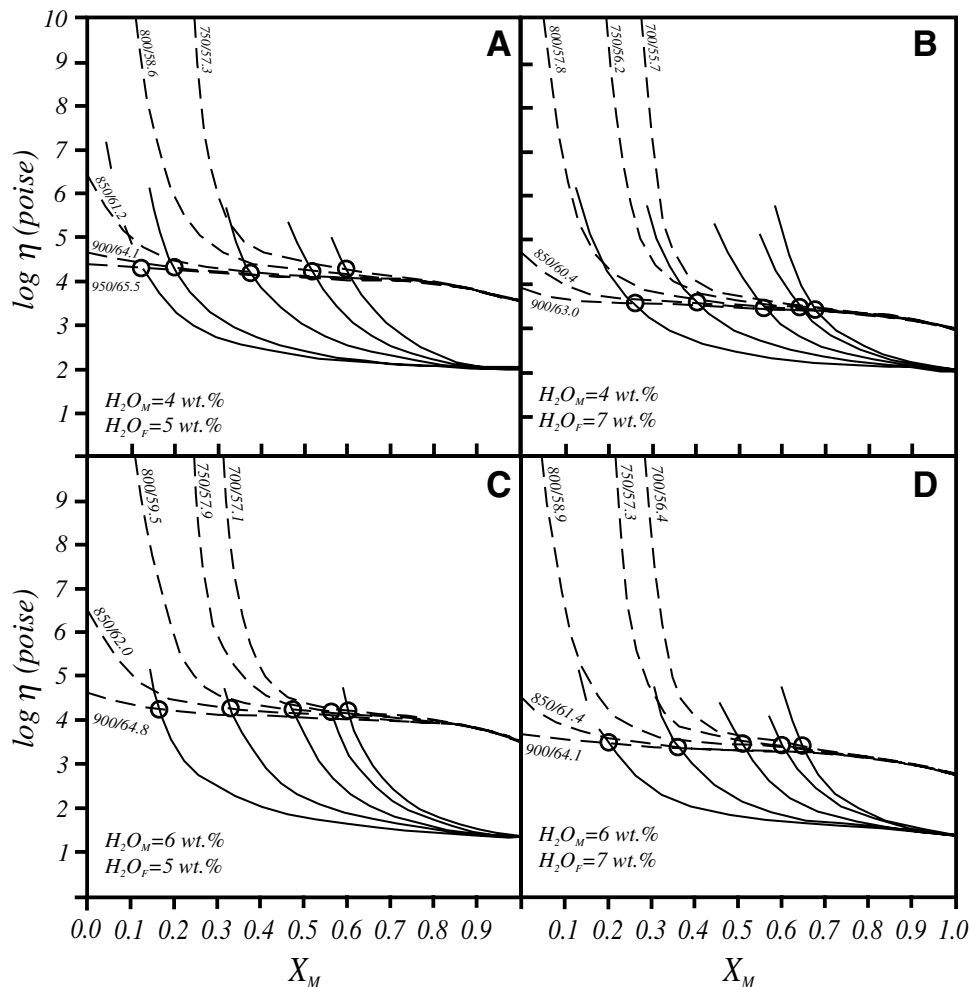


Figure 14. Viscosity-composition diagram for enclave (diortite)-host pairs in a late-stage tonalitic dike, showing the variations in viscosity and composition of hybrid magmas as a function of initial temperatures and H_2O contents of the enclave (solid curves) and host (dashed curves) magmas. Each panel in the figure represents different conditions of initial H_2O contents in the enclave (H_2O_M) and host (H_2O_F) magmas. The dashed curves in each panel are labeled X/Y, where X is the initial temperature (in $^{\circ}C$) of the host magma and Y is the SiO_2 content (in wt%) of the resultant hybrid.

balance calculations (see discussion above), mixing at $\hat{\eta}$ requires host magma temperatures of 775–800 $^{\circ}C$ for initial H_2O contents of 4–6 wt%.

Additional calculations were performed to evaluate the conditions and extent of mixing between the hybrid andesitic and host granodioritic magmas, the results of which are shown in Figure 13. The initial temperature and H_2O content of the andesitic end-member were taken from results of the basalt-granodiorite mixing calculations (see above). Intersections between curves representing the andesitic and granodioritic end-members ($\hat{\eta}$) occur at higher viscosities ($10^{4.6}$ – $10^{5.8}$ poise; Fig. 13) than those between basaltic and granodioritic magmas ($<10^5$ poise; Fig. 12). In addition, mixing between andesitic and granodioritic magmas at $\hat{\eta}$ could only occur at $X_M > 0.60$, which is significantly greater than the $X_M \sim 0.18$ predicted by major element mass balance. These results indicate that conditions suitable for complete binary mixing of andesitic and granodioritic magmas in the late-stage granodioritic dikes were never achieved and that the dark-colored granodiorite adjacent to the andesitic enclaves was instead produced by diffusion of chemical components across the enclave-host contact.

Late-Stage Tonalitic Dikes. Mixing results for the late-stage tonalitic dikes are more difficult to assess, because the hybrid compositions span a wide range in compositions. The hornblende-rich nature of the microdiortitic enclaves suggests relatively high H_2O contents of 3–6 wt% (Sisson and Grove, 1993); the low An content of plagioclase suggests, however, that the H_2O content was at the low end of the range (Sisson and Grove, 1993). The lack of orthopyroxene and the abundance of early biotite in the tonalitic rocks suggest that the felsic magma was H_2O -rich, but not H_2O -saturated (5–7 wt% H_2O ; Scaillet and Evans, 1999). Calculations were performed using a range of host magma H_2O contents (5.0–7.0 wt%) and initial temperatures (700–950 $^{\circ}C$) and using an enclave magma H_2O content of 4.0 wt% (Fig. 14). An increase in host magma H_2O content from 5.0 to 7.0 wt% causes a decrease in $\hat{\eta}$ from $10^{4.2}$ to $10^{3.5}$ poise; however, an increase in the enclave magma H_2O content from 4.0 to 6.0 wt% over the same range of host magma H_2O contents (5.0–7.0 wt%) and initial temperatures (750–900 $^{\circ}C$) does not affect $\hat{\eta}$ ($10^{4.3}$ – $10^{3.5}$ poise). Ideal mixing of enclave and host magmas at $\hat{\eta}$ cannot account for the range in hybrid compositions observed in the late-stage tonalitic dikes, particularly those

having $X_M > 0.7$ ($\text{SiO}_2 < 55$ wt%), which is probably a result of accumulation (see above).

The coarser grain size of the microdioritic enclaves, compared to the basaltic enclaves in the granodioritic dikes, suggests that the dioritic magma did not experience the same degree of undercooling or that it was largely crystalline when it came into contact with the tonalitic magma. The former suggests a smaller temperature contrast between mafic and felsic magmas, whereas the latter might indicate a high contrast in initial viscosities. A decrease in the temperature contrast results in mixing at progressively lower X_M (Fig. 14). However, a decrease in the initial viscosity contrast between the two magmas results in ideal mixing at slightly greater values for X_M , but still well below the values suggested by mass-balance calculations (Fig. 14). The bimodal grain size of the hybrid rocks is characteristic of mixing between crystal-rich mushes (e.g., D'Lemos, 1996); therefore, it is unlikely that the hybrid compositions were produced by mixing of liquid magmas having equal viscosities (see Fig. 14).

DISCUSSION

Barnes et al. (1995) documented a great number of mafic rock types in the Grayback pluton. The lithologic heterogeneity observed, even at the hand sample scale, attests to the presence of coexisting magmas throughout main-stage magmatism. The main stage of the pluton comprises gabbro, norite, quartz diorite, and lesser amounts of pyroxenite and tonalite. Coeval calc-alkaline and evolved tholeiitic basaltic magmas point to a heterogeneous mantle source. Barnes et al. (1995) demonstrated that fractional crystallization of plagioclase + magnetite + olivine \pm clinopyroxene \pm orthopyroxene \pm hornblende \pm apatite from calc-alkaline basaltic magma of the main stage could produce felsic compositions similar to those observed in the late-stage granodioritic and granitic dikes. Such a process could explain the abundance of cumulate pyroxenites and melagabbros with $\text{Mg}/(\text{Mg} + \text{Fe}) > 0.58$ (see Barnes et al., 1995).

Fractional crystallization resulted in an initial increase in P_2O_5 , followed by an abrupt decrease at the onset of apatite crystallization (Fig. 5C). In addition, TiO_2 (Fig. 5A), Al_2O_3 , and Sr abundances steadily decreased owing to the removal of Fe-Ti oxides, clinopyroxene, and plagioclase. Few main-stage samples follow the fractional crystallization trend observed in Figure 5, but instead exhibit increasing TiO_2 , Al_2O_3 , P_2O_5 , and Sr with decreasing $\text{Mg}/(\text{Mg} + \text{Fe})$. Likewise, few samples follow the mixing trends exhibited by enclave-host pairs in the late-stage granodioritic and tonalitic dikes. It is difficult to discern a clear liquid line of descent with respect to most elements, but most of the noncumulate main-stage samples plot near the field of enclave and host compositions represented by the Lake Mountain mafic enclave swarm (Fig. 5). The compositional similarities between the Lake Mountain mafic enclave swarm and Grayback main-stage samples suggest that mixing between calc-alkaline basaltic and andesitic magmas occurred throughout much of the Grayback history, probably at a greater depth than represented by the current level of exposure. The enclave

and host magmas observed in the Lake Mountain mafic enclave swarm were prevented from mixing, possibly as a result of devolatilization or a temperature decrease (and hence, a higher crystallinity). A similar scenario could be envisioned for tholeiitic compositions in the mafic enclave swarm on Grayback Mountain, which tapped a distinctly different mantle source (Barnes et al., 1995).

Some basaltic magma evolved to granitic compositions through fractional crystallization. Minor assimilation of meta-sedimentary rocks gave rise to the elevated $^{87}\text{Sr}/^{86}\text{Sr}$ and $\delta^{18}\text{O}$ contents of the granites (Barnes et al., 1992a). Continued influx of basaltic magma and subsequent mixing with the silicic magma produced hybrid andesite, presumably at a deeper level in the Grayback system. Intrusion of the granitic magma to the present level of exposure entrained small volumes of basaltic and andesitic magmas that quickly solidified in their new environment, producing the mafic and intermediate enclaves. Although the late-stage granodioritic dikes lack evidence for extensive mixing between mafic and felsic magmas in situ, the presence of hybrid andesitic enclaves indicates that such mixing did occur in the Grayback system, requiring close to 60% of the basaltic end-member for complete mixing to take place. That the hybrid andesite compositions are unlike any main-stage samples suggests either that the andesite produced in this manner was volumetrically minor or that large volumes did not ascend to the present level of exposure.

Heat from mafic magma partially melted mafic meta-volcanic rocks residing deep in the Klamath crust, generating small volumes of high-Al tonalitic magma. Major and trace element signatures of the tonalitic rocks (high Al_2O_3 and Na_2O , and low K_2O , Y, and HREE; Drummond and Defant, 1990) suggest that partial melting occurred in equilibrium with a garnet- and hornblende-bearing residual assemblage at pressures exceeding 10 kb (Wolf and Wyllie, 1994; Rapp and Watson, 1995). Injection of calc-alkaline basaltic magma into the high-Al tonalitic magma resulted in limited mixing and the magma mingling relationships observed in the late-stage tonalitic dikes. Results of this study indicate that this basalt-tonalite mixing did not play a significant role in the compositional variation of the Grayback main stage.

Other plutons in the Wooley Creek belt experienced open-system behavior similar to the Grayback pluton. In the Wooley Creek batholith, basalt mixed with fractionated dacite in the upper part of the magma chamber to produce hybrid andesite (Barnes et al., 1986, 1987). Open-system behavior in the Ashland pluton (Gribble et al., 1990) led to mixing between alkalic basalt and tonalite and resultant quartz monzodioritic magma, which evolved by coupled fractionation and assimilation to more felsic compositions. Schmidt (1994) determined that mixing between andesitic magma and anatectic granodiorite and granite was important during later stages of the composite English Peak pluton. In addition, mafic enclaves throughout the Russian Peak pluton indicate not only the presence of mafic magma in the system but, coupled with ranges in Sr and O isotope abundances (Cotkin and Medaris, 1993), hint at the possible role of magma mixing in its

history. The Grayback pluton, however, is unusual amongst these plutons in that mafic magmas from multiple mantle sources were prevalent *throughout* its history. It is likely that ascent of mantle-derived magmas into the Grayback system was facilitated by extension in the back-arc of the contemporaneous Rogue–Chetco arc complex (Harper et al., 1994). This setting, directly inboard of the arc, may have experienced greater extension than further inboard or to the south, positions currently occupied by the other Wooley Creek belt plutons.

CONCLUSIONS

A diverse range of magma-mingling zones in the Grayback pluton provides valuable information about the physicochemical interactions of magmas, and documents the coexistence of several mantle-derived magmas throughout the evolution of the Grayback system. Comparisons between rock compositions preserved in the magma-mingling zones and those from the main stage of the pluton suggest that most of the compositional variation within the Grayback pluton resulted from mixing of calc-alkaline basaltic and andesitic magmas. Late-stage activity resulted in the emplacement of enclave-bearing granodioritic and tonalitic dikes, which exhibit different styles of interaction between mafic and felsic end-members.

Grayback magmatism was coeval with other plutons of the Wooley Creek belt, which all show evidence for a significant role for mafic magmas in their evolution. Increased interaction of mantle-derived magmas and crustal rocks in Wooley Creek belt plutonic systems, compared with earlier episodes of Jurassic magmatism, was facilitated by extension in the back-arc region of a contemporaneous volcanic arc. Emplacement of these mafic magmas into already-warmed crust allowed for assimilation of crustal rocks and/or mixing with anatectic melts.

ACKNOWLEDGMENTS

We are pleased to have the opportunity to contribute to this volume honoring Porter Irwin's pioneering and influential work in the Klamath Mountains. We thank Bennetta Schmidt and Melanie Barnes for help in the field, and Bill Shannon and Melanie for their invaluable assistance in the laboratory. We appreciate the thorough and constructive reviews of Nancy McMillan and Daniel Lux. Funding was provided by a Penrose Bequest of the Geological Society of America (KJ) and National Science Foundation grants EAR-8720141 and EAR-9117103 (CGB).

REFERENCES CITED

- Allen, C.M., and Barnes, C.G., 2006, this volume, Ages and some cryptic sources of Mesozoic plutonic rocks in the Klamath Mountains, California and Oregon, in Snoke, A.W., and Barnes, C.G., eds., Geological studies in the Klamath Mountains province, California and Oregon: A volume in honor of William P. Irwin: Boulder, Colorado, Geological Society of America Special Paper 410, doi: 10.1130/2006.2410(11).
- Barker, F., 1979, Trondhjemite: Definition, environment, and hypotheses of origin, in Barker, F., ed., Trondhjemites, dacites, and related rocks: Amsterdam, Elsevier, p. 1–12.
- Barnes, C.G., 1983, Petrology and upward zonation of the Wooley Creek batholith, Klamath Mountains, California: *Journal of Petrology*, v. 24, p. 495–537.
- Barnes, C.G., Allen, C.M., and Saleeby, J.B., 1986, Open- and closed-system characteristics of a tilted plutonic system, Klamath Mountains, California: *Journal of Geophysical Research*, v. 91, p. 6073–6090.
- Barnes, C.G., Allen, C.M., and Brigham, R.H., 1987, Isotopic heterogeneity in a tilted plutonic system, Klamath Mountains, California: *Geology*, v. 15, p. 523–527, doi: 10.1130/0091-7613(1987)15<523:IHIA TP>2.0.CO;2.
- Barnes, C.G., Petersen, S.W., Kistler, R.W., Prestvik, T., and Sundvoll, B., 1992a, Tectonic implications of isotopic variation among Jurassic and Early Cretaceous plutons, Klamath Mountains: *Geological Society of America Bulletin*, v. 104, p. 117–126, doi: 10.1130/0016-7606(1992)104<0117:TIOIVA>2.3.CO;2.
- Barnes, C.G., Barnes, M.A., and Kistler, R.W., 1992b, Petrology of the Caribou Mountain pluton, Klamath Mountains, California: *Journal of Petrology*, v. 33, p. 95–124.
- Barnes, C.G., Johnson, K., Barnes, M.A., Prestvik, T., Kistler, R.W., and Sundvoll, B., 1995, The Grayback pluton: Magmatism in a Jurassic back-arc environment, Klamath Mountains, Oregon: *Journal of Petrology*, v. 36, p. 397–416.
- Barnes, C.G., Petersen, S.W., Kistler, R.W., Murray, R., and Kays, M.A., 1996, Source and tectonic implications of tonalite-trondhjemite magmatism in the Klamath Mountains: *Contributions to Mineralogy and Petrology*, v. 123, p. 40–60, doi: 10.1007/s004100050142.
- Barnes, C.G., Mars, E.V., Swapp, S., and Frost, C.D., 2006, this volume (Chapter 10), Petrology and geochemistry of the Middle Jurassic Ironside Mountain batholith: Evolution of potassic magmas in a primitive arc setting, in Snoke, A.W., and Barnes, C.G., eds., Geological studies in the Klamath Mountains province, California and Oregon: A volume in honor of William P. Irwin: Boulder, Colorado, Geological Society of America Special Paper 410, doi: 10.1130/2006.2410(10).
- Castro, A., de la Rosa, J.D., and Stephens, W.E., 1990, Magma mixing in the subvolcanic environment: Petrology of the Gerena interaction zone near Seville, Spain: *Contributions to Mineralogy and Petrology*, v. 106, p. 9–26, doi: 10.1007/BF00306405.
- Cotkin, S.J., and Medaris, L.G., Jr., 1993, Evaluation of the crystallization conditions for the calc-alkaline Russian Peak Intrusive Complex, Klamath Mountains, northern California: *Journal of Petrology*, v. 34, p. 543–571.
- D'Lemos, R.S., 1996, Mixing between granitic and dioritic crystal mushes, Guernsey, Channel Islands, UK: *Lithos*, v. 38, p. 233–257, doi: 10.1016/0024-4937(96)00007-2.
- Donato, M.M., Barnes, C.G., and Tomlinson, S.L., 1996, The enigmatic Applegate Group of southwestern Oregon: Age, correlation, and tectonic affinity: *Oregon Geology*, v. 58, p. 79–91.
- Drummond, M.S., and Defant, M.J., 1990, A model for trondhjemite-tonalite-dacite genesis and crustal growth via slab melting: Archean to modern comparisons: *Journal of Geophysical Research*, v. 95, p. 21,503–21,521.
- Eggler, D.H., 1972, Amphibole stability in H₂O-undersaturated calc-alkaline melts: *Earth and Planetary Science Letters*, v. 15, p. 28–34, doi: 10.1016/0012-821X(72)90025-8.
- Ernst, W.G., 1998, Geology of the Sawyers Bar area, Klamath Mountains, northern California: Sacramento, California Division of Mines and Geology Map Sheet 47, scale 1:48,000, 59 p.
- Frost, T.P., and Lindsay, J.R., 1988, MAGMIX: A BASIC program to calculate viscosities of interacting magmas of differing composition, temperature, and water content: *Computers & Geosciences*, v. 14, p. 213–228, doi: 10.1016/0098-3004(88)90005-2.
- Frost, T.P., and Mahood, G.A., 1987, Field, chemical, and physical constraints on mafic-felsic magma interaction in the Lamarck Granodiorite, Sierra Nevada, California: *Geological Society of America Bulletin*, v. 99, p. 272–291, doi: 10.1130/0016-7606(1987)99<272:FCAPCO>2.0.CO;2.
- Garcia, M.O., 1982, Petrology of the Rogue River island-arc complex, southwest Oregon: *American Journal of Science*, v. 282, p. 783–807.

- Godchaux, M.M., 1969, Petrology of the Grayback Igneous Complex and contact aureole, Klamath Mountains, southwestern Oregon [Ph.D. dissertation]: Eugene, University of Oregon, 223 p.
- Gribble, R.F., Barnes, C.G., Donato, M.M., Hoover, J.D., and Kistler, R.W., 1990, Geochemistry and intrusive history of the Ashland pluton, Klamath Mountains, California and Oregon: *Journal of Petrology*, v. 31, p. 883–923.
- Hacker, B.R., Donato, M.M., Barnes, C.G., McWilliams, M.O., and Ernst, W.G., 1995, Timescales of orogeny: Jurassic construction of the Klamath Mountains: *Tectonics*, v. 14, p. 677–703, doi: 10.1029/94TC02454.
- Harper, G.D., and Wright, J.E., 1984, Middle to Late Jurassic tectonic evolution of the Klamath Mountains, California-Oregon: *Tectonics*, v. 3, p. 759–772.
- Harper, G.D., Saleeby, J.B., and Heizler, M., 1994, Formation and emplacement of the Josephine ophiolite and the Nevadan orogeny in the Klamath Mountains, California-Oregon: U/Pb zircon and $^{40}\text{Ar}/^{39}\text{Ar}$ geochronology: *Journal of Geophysical Research*, v. 99, p. 4293–4321, doi: 10.1029/93JB02061.
- Haskin, L.A., Haskin, M.A., Frey, F.A., and Wildeman, T.R., 1968, Relative and absolute abundances of the rare earths, in Ahrens, L.H., ed., *Origin and distribution of the elements*: Oxford, Pergamon Press, p. 889–912.
- Hotz, P.E., 1971, Plutonic rocks of the Klamath Mountains, California and Oregon: Washington, D.C., U.S. Geological Survey Professional Paper 684-B, 20 p.
- Irwin, W.P., 1972, Terranes of the western Paleozoic and Triassic belt in the southern Klamath Mountains, California: Washington, D.C., U.S. Geological Survey Professional Paper 800-C, p. 103–111.
- Irwin, W.P., 1981, Tectonic accretion of the Klamath Mountains, in Ernst, W.G., ed., *The geotectonic development of California—Rubey volume 1: Englewood Cliffs, New Jersey, Prentice-Hall*, p. 29–49.
- Irwin, W.P., 1985, Age and tectonics of plutonic belts in accreted terranes of the Klamath Mountains, California and Oregon, in Howell, D.G., ed., *Tectonostratigraphic terranes of the Circum-Pacific Region*: Houston, Circum-Pacific Council for Energy and Mineral Resources, Earth Science Series 1, p. 187–199.
- Irwin, W.P., and Wooden, J., 1999, Plutons and accretionary episodes of the Klamath Mountains, California and Oregon: Reston, Virginia, U.S. Geological Survey Open-File Report 99-374, 1 sheet.
- Johnson, K., 1991, Magma mixing and mingling in the Grayback pluton, Klamath Mountains, southwest Oregon [M.S. thesis]: Lubbock, Texas Tech University, 122 p.
- Koyaguchi, T., 1986, Evidence for two-stage mixing in magmatic inclusions and rhyolitic lava domes on Nijima Island, Japan: *Journal of Volcanology and Geothermal Research*, v. 29, p. 71–98, doi: 10.1016/0377-0273(86)90040-5.
- Kuritani, T., Yokoyama, T., Kobayashi, K., and Nakamura, E., 2003, Shift and rotation of composition trends by magma mixing: 1983 eruption of Miyake-jima volcano, Japan: *Journal of Petrology*, v. 44, p. 1895–1916, doi: 10.1093/petrology/egg063.
- Langmuir, C.H., Vocke, R.D., Hanson, G.N., and Hart, S.R., 1978, A general mixing equation with applications to Icelandic basalts: *Earth and Planetary Science Letters*, v. 37, p. 380–392, doi: 10.1016/0012-821X(78)90053-5.
- Marshall, L.A., and Sparks, R.S.J., 1984, Origin of some mixed-magma and net-veined ring intrusions: *Journal of the Geological Society (London)*, v. 141, p. 171–182.
- Naney, M.T., 1983, Phase equilibria of rock-forming ferromagnesian silicates in granitic systems: *American Journal of Science*, v. 283, p. 993–1033.
- Perugini, D., and Poli, G., 2004, Analysis and numerical simulation of chaotic advection and chemical diffusion during magma mixing: Petrologic implications: *Lithos*, v. 78, p. 43–66, doi: 10.1016/j.lithos.2004.04.039.
- Rapp, R.P., and Watson, E.B., 1995, Dehydration melting of metabasalt at 8–32 kbar: Implications for continental growth and crust-mantle recycling: *Journal of Petrology*, v. 36, p. 891–931.
- Saleeby, J.B., Harper, G.D., Snoke, A.W., and Sharp, W.D., 1982, Time relations and structural-stratigraphic patterns in ophiolite accretion, west-central Klamath Mountains, California: *Journal of Geophysical Research B*, v. 87, p. 3831–3848.
- Scaillet, B., and Evans, B.W., 1999, The 15 June 1991 eruption of Mount Pinatubo. I. Phase equilibria and pre-eruption P–T–fO₂–fH₂O conditions of the dacite magma: *Journal of Petrology*, v. 40, p. 381–411, doi: 10.1093/petrology/40.3.381.
- Schmidt, B.L., 1994, The petrology and geochemistry of the English Peak intrusive suite, Klamath Mountains, California [Ph.D. dissertation]: Lubbock, Texas Tech University, 216 p.
- Shannon, W.M., 1994, Petrogenesis of Middle Proterozoic alkaline granitic rocks, Franklin Mountains, west Texas [Ph.D. dissertation]: Lubbock, Texas Tech University, 240 p.
- Sisson, T.W., and Grove, T.L., 1993, Experimental investigations of the role of H₂O in calc-alkaline differentiation and subduction zone magmatism: *Contributions to Mineralogy and Petrology*, v. 113, p. 143–166, doi: 10.1007/BF00283225.
- Smith, E.I., Feuerbach, D.L., Naumann, T.R., and Mills, J.G., 1990, Mid-Miocene volcanic and plutonic rocks in the Lake Mead area of Nevada and Arizona: Production of intermediate igneous rocks in an extensional environment, in Anderson, J.L., ed., *The nature and origin of Cordilleran magmatism*: Boulder, Colorado, Geological Society of America Memoir 174, p. 169–194.
- Sparks, R.S.J., and Marshall, L.A., 1986, Thermal and mechanical constraints on mixing between mafic and silicic magmas: *Journal of Volcanology and Geothermal Research*, v. 29, p. 99–124, doi: 10.1016/0377-0273(86)90041-7.
- Vernon, R.H., 1983, Restite, xenoliths, and microgranitoid enclaves in granites: *Journal and Proceedings, Royal Society of New South Wales*, v. 166, p. 77–103.
- Vogel, T.A., 1982, Magma mixing in the acidic-basic complex of Ardnamurchan: Implications on the evolution of shallow magma chambers: *Contributions to Mineralogy and Petrology*, v. 79, p. 411–423, doi: 10.1007/BF01132071.
- Watson, E.B., and Jurewicz, S.R., 1984, Behavior of alkalis during diffusive interaction of granitic xenoliths with basaltic magma: *Journal of Geology*, v. 92, p. 121–131.
- Wiebe, R.A., 1991, Commingling of contrasted magmas and generation of mafic enclaves in granitic rocks, in Didier, J., and Barbarin, B., eds., *Enclaves and granite petrology*: Amsterdam, Elsevier, *Developments in Petrology* 13, p. 393–402.
- Wiebe, R.A., Frey, H., and Hawkins, D.P., 2001, Basaltic pillow mounds in the Vinalhaven intrusion, Maine: *Journal of Volcanology and Geothermal Research*, v. 107, p. 171–184, doi: 10.1016/S0377-0273(00)00253-5.
- Wiebe, R.A., Blair, K.D., Hawkins, D.P., and Sabine, C.P., 2002, Mafic injections, in situ hybridization, and crystal accumulation in the Pyramid Peak granite, California: *Geological Society of America Bulletin*, v. 114, p. 909–920, doi: 10.1130/0016-7606(2002)114<0909:MIISHA>2.0.CO;2.
- Wolf, M.B., and Wyllie, P.J., 1994, Dehydration-melting of amphibolite at 10 kbar: The effects of temperature and time: *Contributions to Mineralogy and Petrology*, v. 115, p. 369–383, doi: 10.1007/BF00320972.
- Wood, D.A., 1978, Major and trace element variations in the Tertiary lavas of eastern Iceland and their significance with respect to the Iceland geochemical anomaly: *Journal of Petrology*, v. 19, p. 393–436.
- Wyld, S.J., and Wright, J.E., 1988, The Devils Elbow ophiolite remnant and overlying Galice Formation: New constraints on the Middle to Late Jurassic evolution of the Klamath Mountains, California: *Geological Society of America Bulletin*, v. 100, p. 29–44, doi: 10.1130/0016-7606(1988)100<0029:TDEORA>2.3.CO;2.
- Yule, J.D., Saleeby, J.B., and Barnes, C.G., 2006, this volume, A rift-edge facies of the Late Jurassic Rogue–Chetco arc and Josephine ophiolite, Klamath Mountains, Oregon, in Snoke, A.W., and Barnes, C.G., eds., *Geological studies in the Klamath Mountains province, California and Oregon: A volume in honor of William P. Irwin*: Boulder, Colorado, Geological Society of America Special Paper 410, doi: 10.1130/2006.2410(03).

